Title page

Fgf10 is required for specification of non-sensory regions of the cochlear epithelium

Lisa D. Urness[a], Xiaofen Wang[a], Shumei Shibata[b,1], Takahiro Ohyama[b] and Suzanne L. Mansour[a,c]

[a]Department of Human Genetics, University of Utah, Salt Lake City, UT 84112; [b]Department of Otolaryngology-Head & Neck Surgery and Zilkha Neurogenetic Institute, Keck School of Medicine, University of Southern California, Los Angeles, CA 90033; [c]Department of Neurobiology & Anatomy, University of Utah, Salt Lake City, UT 84132

Corresponding Author:

Suzanne L. Mansour

Department of Human Genetics

University of Utah

15 North, 2030 East, Room 2100

Salt Lake City, UT 84112-5330

Phone: +1-801-585-6893

e-mail: suzi.mansour@genetics.utah.edu

[1]Present address: Department of Otorhinolaryngology, Graduate School of Medical Sciences, Kyushu University, 812-8582 Fukuoka, Japan

UU IR Author Manuscript

Abstract

The vertebrate inner ear is a morphologically complex sensory organ comprised of two compartments, the dorsal vestibular apparatus and the ventral cochlear duct, required for motion and sound detection, respectively. *Fgf10*, in addition to *Fgf3*, is necessary for the earliest stage of otic placode induction, but continued expression of *Fgf10* in the developing otic epithelium, including the prosensory domain and later in Kolliker's organ, suggests additional roles for this gene during morphogenesis of the labyrinth. While loss of *Fgf10* was implicated previously in semicircular canal agenesis, we show that $Fgf10^{-/+}$ embryos also exhibit a reduction or absence of the posterior semicircular canal, revealing a dosage-sensitive requirement for FGF10 in vestibular development. In addition, we show that $Fgf10^{-/-}$ embryos have previously unappreciated defects of cochlear morphogenesis, including a somewhat shortened duct, and, surprisingly, a substantially narrower duct. The mutant cochlear epithelium lacks Reissner's membrane and a large portion of the outer sulcus--two non-contiguous, non-sensory domains. Marker gene analyses revealed effects on Reissner's membrane as early as E12.5-E13.5 and on the outer sulcus by E15.5, stages when *Fgf10* is expressed in close proximity to *Fgfr2b*, but these effects were not accompanied by changes in epithelial cell proliferation or death. These data indicate a dual role for *Fgf10* in cochlear development: to regulate outgrowth of the duct and subsequently as a bidirectional signal that sequentially specifies Reissner's membrane and outer sulcus non-sensory domains. These findings may help to explain the hearing loss sometimes observed in LADD syndrome subjects with *FGF10* mutations.

Keywords **FGF signaling; cochlea; Reissner's membrane; outer sulcus**

UU IR Author Manuscript

Highlights--Urness et al.

- *Fgf10* has a dosage-sensitive role in vestibular morphogenesis
- *Fgf10* is required for cochlear morphogenesis
- *Fgf10* null mutants lack Reissner's membrane and are deficient in outer sulcus tissue
- FGF10 signals sequentially and bi-directionally to specify these non-sensory domains

Graphical Abstract—Urness et al.

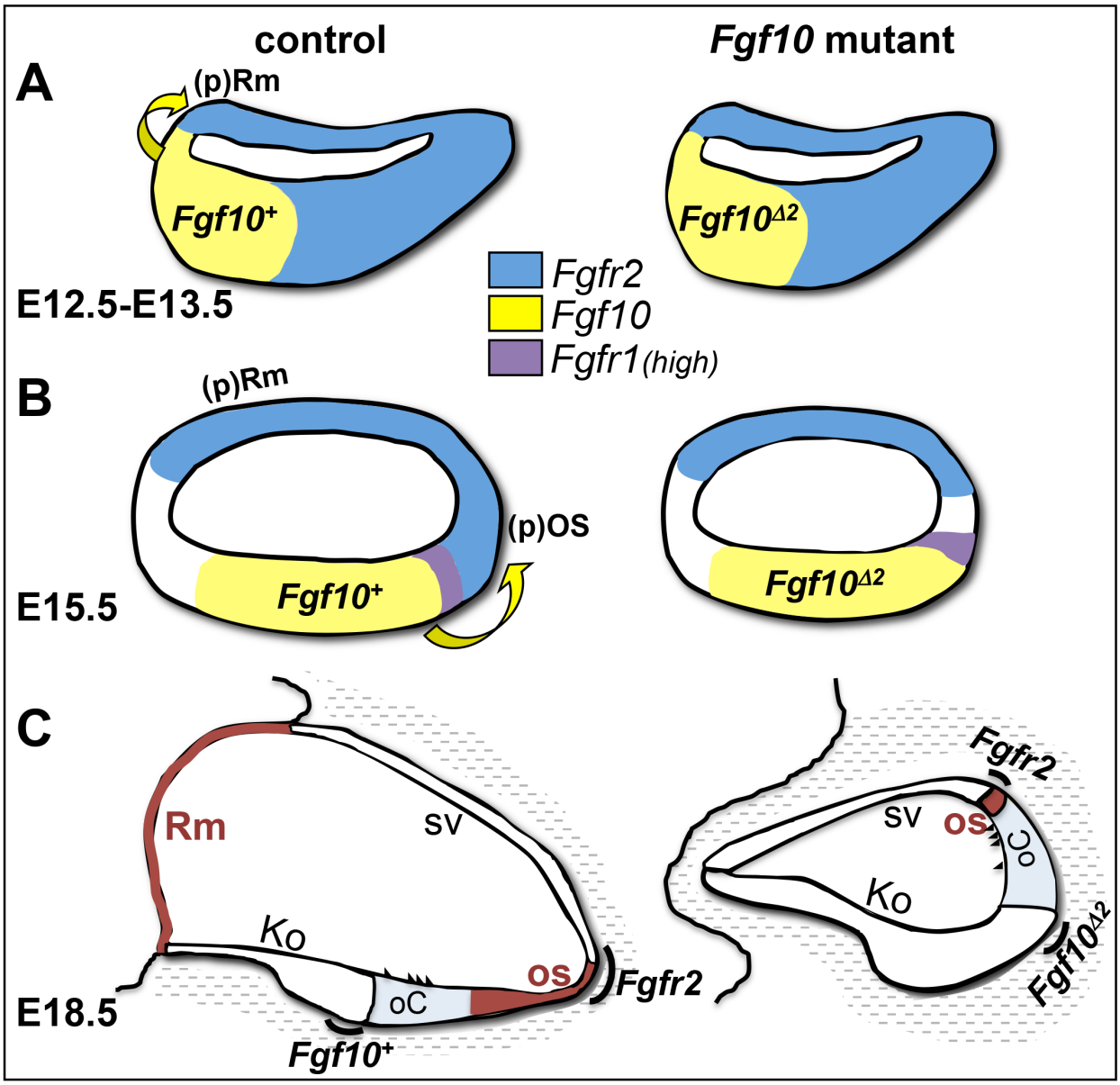

UU IR Author Manuscript

Introduction

The mammalian inner ear is a morphologically complex sensory organ with two functionally distinct compartments, the ventral auditory and dorsal vestibular divisions, which are responsible for the perception of sound and movement, respectively. The auditory compartment, the cochlea, derives from a ventral outgrowth of the otic vesicle epithelium, which undergoes progressive extension and, in mammals, coils as it matures. Vestibular structures derive from dorsal and lateral evaginations of the otic epithelium and are sculpted into the three semicircular canals used to detect angular acceleration, as well as two central pouches, the utricle and saccule, used to detect linear acceleration. The inner ear epithelium also has a dorsally projecting non-sensory appendage, the endolymphatic duct and sac, which maintains the unique ionic composition of the endolymph fluid in the inner ear lumen and is essential for normal sensory functions (Groves and Fekete, 2012; Wu and Kelley, 2012).

Gross morphogenesis of the inner ear epithelium is largely complete by E15.5 in the mouse (Morsli et al., 1998), at which time the cochlea has achieved 1.75 turns and remodeling of dorsal orthogonal epithelial pouches has resulted in formation of the three patent semicircular canals (see Fig. 1A). Differentiation of the epithelium into distinct sensory and non-sensory domains with their characteristic cell types occurs concomitantly with gross morphogenesis and is not complete until well after birth in mouse. Although many human sensorineural deafness and balance disorders are caused by genetic or environmental insults that affect the function of particular inner ear cell types and are not detectable radiologically, almost 40% of inner ear dysfunction may be accompanied by congenital malformation of the epithelium (Mafong et al., 2002; Wu et al., 2005) and the presence of malformations impacts treatment plans. Therefore, to

advance both treatment and ultimately prevention, it is essential to elucidate the functions of signals controlling otic morphogenesis.

Genetic analyses show that FGF signaling is particularly important for inner ear morphogenesis. Multiple FGFs functioning from nearby tissues induce formation of the otic placode in posterior head ectoderm (Alvarez et al., 2003; Ladher et al., 2005; Wright and Mansour, 2003; Zelarayan et al., 2007). The otic placode then invaginates and closes, forming the spherical otic vesicle. Several FGFs, whether signaling from the nearby hindbrain (FGF3) or from within the otic epithelium itself (FGF3, FGF9 and FGF10) are required for subsequent morphogenesis of the dorsal otic vesicle. Mice that lack *Fgf3* function fail with variable penetrance and expressivity to form an endolymphatic duct and the affected otic vesicles develop variably, with impacts on both vestibular and cochlear morphogenesis and function (Hatch et al., 2007; Mansour et al., 1993). The relative contributions of hindbrain and otic epithelial *Fgf3* to these phenotypes have not been determined.

Mice lacking *Fgf9*, which is expressed in non-sensory domains of both the vestibular and cochlear epithelia, have severe abnormalities of vestibular morphogenesis. Semicircular canals are absent or rudimentary and these phenotypes are thought to arise from disrupted communication between the otic epithelium and the surrounding mesenchyme. The cochlear abnormalities of *Fgf9* mutants are subtle. The cochlear epithelium appears relatively normal, but mesothelial cells adjacent to the epithelial component of Reissner's membrane, which is normally a site of *Fgf9* expression, fail to attach to the membrane and the adjacent scala vestibuli (a channel cleared of mesenchyme and filled with perilymph) is enlarged. This is consistent with a disruption of epithelial/mesenchymal communication (Pirvola et al., 2004).

UU IR Author Manuscript

Finally, mice lacking *Fgf10*, which is expressed in both vestibular and cochlear prosensory epithelial tissue as well as in the developing otic ganglion, show complete agenesis of the posterior sensory and non-sensory vestibular tissue (crista and posterior semicircular canal, respectively), and have milder deformations of the anterior and lateral cristae and their associated semicircular canals. The otic ganglion forms normally, but innervation of the vestibular system is disrupted, presumably due to the absence of targets (Ohuchi et al., 2005; Pauley et al., 2003). In contrast, no specific abnormalities of cochlear histogenesis or morphogenesis were described, although Pauley et al. (2003) noted a slight shortening of the cochlear duct. The individual contributions of otic ganglion vs. epithelial sources of *Fgf10* are unknown.

As a prelude to studies dissecting the individual and combinatorial requirements for epithelial *Fgf3* and *Fgf10* in mouse otic morphogenesis, we observed that global *Fgf10* heterozygous inner ears also presented with vestibular defects (a small or absent posterior semicircular canal). Furthermore, the *Fgf10* homozygous null mutant cochlear duct was noticeably shorter and, most surprisingly, narrower than that of heterozygous or wild type littermates. Histologic and marker analyses revealed that while the cochlear sensory domain and two non-sensory domains, Kolliker's organ (the inner sulcus) and the stria vascularis, appeared to develop normally, epithelial tissue in two other non-contiguous non-sensory domains was deleted; namely, all of Reissner's membrane and a substantial portion of the outer sulcus. Analysis of molecular markers during development showed that the Reissner's membrane defect preceded the outer sulcus defect, and that both could be correlated to loss of signaling from FGF10 to its major receptor, FGFR2b, at times when the ligand and receptor were in close proximity. However, we did not detect differences between controls and mutants with respect to proliferation or cell death. Taken together, these data demonstrate a previously unappreciated

UU IR Author Manuscript

role for cochlear FGF10 as a bi-directional signal that promotes sequential specification of non-contiguous non-sensory domains of the cochlear epithelium. This is the first report of such a signal and our findings have implications for understanding the hearing loss of LADD syndrome individuals bearing mutations in *FGF10*.

Materials and methods

These studies complied with protocols approved by the University of Utah Institutional Animal Care and Use Committee.

Generation of Fgf10 null embryos

Generation and PCR genotyping of the *Fgf10* null allele (*Fgf10*$^{-}$, also known as *Fgf10*$^{\Delta 2}$ and formally designated *Fgf10*$^{tm1.1Sms}$; MGI:3526181) were described previously (Urness et al., 2010). *Fgf10*$^{-/+}$ mice were maintained on a mixed genetic background comprised of C57Bl/6 and various 129 substrains. *Fgf10*$^{-/+}$ adults were intercrossed and noon of the day on which a mating plug was observed was designated as E0.5.

Paintfilling of embryonic inner ears

E11.5-E15.5 embryos were fixed in Bodian's solution, dehydrated in ethanol, cleared with methyl salicylate and the inner ear lumens filled with white latex paint as described (Kiernan, 2006; Morsli et al., 1998). Filled ears were roughly dissected and photographed under darkfield illumination using a QImaging Micropublisher digital camera mounted on a Zeiss Discovery V.12 microscope.

UU IR Author Manuscript

RNA in situ hybridization to paraffin sections

Heads of E12.5-E18.5 intercross embryos were fixed in modified Carnoy's solution, embedded in paraffin (Paraplast X-tra) and 10 μm sections were dewaxed, blocked and hybridized with digoxigenin-labeled anti-sense RNA probes, which were detected with alkaline-phosphatase conjugated anti-digoxigenin antibodies as described (Urness et al., 2008). Probes for *Fgf10*, *Myo6*, *Lgr5*, *Fgfr1*, *Spry2*, *Spry1*, *Bmp4*, *Fgfr2*, *Fgf9*, and *Lnfg* were generated by transcription of cDNA-containing plasmids. A list of the template plasmids and acknowledgements is found in Supplementary Table 1. The rest of the RNA probes were generated by transcription of a PCR-amplified, gene-specific 3' UTR fragment containing a T7 promoter. The primer sequences can be found in Supplementary Table 2.

Immunofluorescence analysis of inner ear frozen sections

Whole E18.5 heads were bisected in the sagittal or transverse plane and fixed for 2 hours at room temperature in 4% paraformaldehyde prepared in phosphate buffered saline (PBS). Heads were cryoprotected and embedded in sucrose/gelatin as described (Hurley et al., 2003) with the following modifications: 5% sucrose infiltration overnight at 4°C, 15% sucrose infiltration overnight at 4°C, 15% sucrose/7.5% gelatin (Bloom 300, Sigma G2500) infiltration at 37°C overnight. Samples were cryosectioned at 10 μm thickness (6 μm for proliferation studies) in the sagittal plane, collected on SuperFrost Plus slides and stored at -20°C. Primary antibodies were diluted into PBS/5% normal serum of the secondary antibody species/0.2% Triton X-100 and applied at the following dilutions: mouse anti-p27[Kip1] (BD Biosciences #610241), 1:300; rat anti-CD44 (BD Biosciences #550538), 1:800; rabbit anti-MYO7A (Proteus Biosciences #25-

UU IR Author Manuscript

6790), 1:800; goat anti-SOX2 (Santa Cruz Biotechnology #sc-17320), 1:200; rabbit anti-S100 (Millipore #07-476), 1:1000; rabbit anti-cleaved Caspase-3 (Cell Signaling 9661), 1:100; rabbit anti-phospho-Histone H3 (Millipore 06-570), 1:400. Permeabilization was enhanced by one hr incubation in PBS/1% deoxycholate/0.2% Triton X-100 at room temperature. Secondary antibodies were all from Invitrogen and diluted 1:350 into PBST/5% normal serum (Alexa Fluor® 594 goat anti-rat (A11007); Alexa Fluor® 488 goat anti-rabbit (A11034); and Alexa Fluor® 594 donkey anti-goat (A11058) Alexa Fluor® 488 donkey anti-goat (A11055); Alexa Fluor® 488 donkey anti-rabbit (A21206). DAPI was included in the mounting medium (Vectashield, Vector Labs) and fluorescent signal channels were overlaid using Photoshop CS4.

Analysis of cochlear duct proliferation

Pregnant dams (E13.5) were injected once with BrdU solution (50 μg/g body weight, Invitrogen 00-0103), harvested one hour later and fixed overnight in 4% PFA. Heads were infiltrated with sucrose/gelatin and 6 μm cryosections prepared as described above. DNA was denatured by incubating the slides in 1N HCl at 48° for 30 minutes, followed by neutralization in PBS. BrdU was detected as described above using a mouse monoclonal antibody, MoBu-1 (Invitrogen B35128) at 1:100 and Alexa Fluor® 594 goat anti-mouse (Invitrogen A11032). For analysis at E11.5, cryosections were prepared and phospho-Histone H3 was detected as described above. To differentiate between sensory and non-sensory duct domains, we co-stained the sections to detect SOX2 also as described above. E11.5 data came from 8 sections in each of 6 controls and 6 *Fgf10* null mutants. E13.5 data came from 5 sections in each of 4 controls and 4 *Fgf10* null mutants. Student's t-test (unpaired, two-tailed; Prism 6.0) was used to compare the mean number of BrdU or phospho-Histone H3-positive cells per unit area in control and $Fgf10^{-/-}$

UU IR Author Manuscript

samples. SOX2-positive and SOX2-negative domains were considered separately.

Cochlear duct cross-sectional area analysis

For the E18.5 measurements of the three scalae, we photographed the cochlea in H&E-stained sagittal sections of the head. Three sections spaced at 50 μm intervals near the center of each of 3 control and 3 *Fgf10*$^{-/-}$ inner ears were analyzed. The AxioVison measurement module (Zeiss) was used to measure the area of each the three scalae in the basal cross section and the three measurements for each sample were averaged. The average area of each scala from the 3 control and 3 mutant samples were compared using multiple t tests. Statistical significance was determined using the Holm-Sidak method (Prism 6.0 software). For E12.5 and E13.5 scala media area measurements, three contiguous sections were photographed from the cochlear base of 3 control and 3 *Fgf10*$^{-/-}$ inner ears sectioned coronally. For E15.5 scala media area measurements, three contiguous images were captured representing the most basal turn. Area measurements were captured and analyzed as described above.

Results

Fgf10 is required for both vestibular and cochlear morphogenesis

It is well known that *Fgf10* is required for morphogenesis of the vestibular system. Specifically, *Fgf10* null inner ears lack posterior sensory and non-sensory tissue (the cristae and semicircular canals, respectively), and have variable defects of anterior and lateral semicircular canal morphogenesis, or appear to have un-fused vertical and lateral canal pouches (Ohuchi et al., 2005; Pauley et al., 2003). The status of the cochlear duct is less clear, with one report of a

UU IR Author Manuscript

somewhat shortened, but otherwise normal cochlea (Pauley et al., 2003) and another report of a cochlea of normal length (Ohuchi et al., 2005). To enable morphologic assessment of multiple inner ears of each *Fgf10* genotype we intercrossed *Fgf10*$^{-/+}$ animals, collected embryos at E15.5 when morphogenesis is virtually complete (Morsli et al., 1998), and paint-filled the inner ear epithelia. Visual inspection revealed five morphologic classes (Fig. 1A-E, Y). All 16 wild type ears were normal (Class 0, Fig. 1A). In contrast, only five of 48 heterozygous inner ears were normal, whereas 32 showed a reduced posterior semicircular canal (pscc; Class 1, Fig. 1B) and 11 virtually lacked the pscc, though the posterior ampulla (pa, housing the posterior crista) was present (Class 2, Fig. 1C). Homozygotes were even more severely affected and fell into two classes. As previously observed by other groups (Ohuchi et al., 2005; Pauley et al., 2003), all 24 *Fgf10*$^{-/-}$ inner ears lacked the posterior ampulla and canal. We also observed small and variable reductions in the lateral and anterior semicircular canals, but these were not quantified. Furthermore, all *Fgf10*$^{-/-}$ inner ears had a variably shortened cochlear duct (cd; ~0.75 to 1.5 turns; Fig. 1D, E). In 15 of 24 *Fgf10*$^{-/-}$ inner ears, the process of canal pouch fusion to make an anterior semicircular canal was complete (Class 3, Fig. 1D), whereas in the other 9 inner ears the remaining portion of the vertical canal pouch (vcp) failed to fuse and clear (Class 4, Fig. 1E). These results revealed dosage sensitive requirements for *Fgf10* in vestibular morphogenesis and an unexpected requirement in cochlear morphogenesis (Fig. 1F).

To determine when the abnormalities seen in *Fgf10*$^{-/+}$ and *Fgf10*$^{-/-}$ inner ears were first apparent, we paint-filled embryonic inner ears from *Fgf10*$^{-/+}$ intercrosses at progressively earlier stages of development. All five previously defined classes (Fig. 1Y) were apparent at both E14.5 (Fig. 1G-K) and E13.5 (Fig. 1M-Q) in proportions roughly similar to those seen at E15.5 (Fig.

UU IR Author Manuscript

1F, L, R). Therefore the vestibular and cochlear abnormalities noted at E15.5 must have initiated before E13.5.

At E12.5, only three morphologic classes were clearly distinguishable and these correlated with genotype. At this stage there was variability across all genotypes with respect to the extent of canal pouch fusion plate clearing and this correlated with overall embryo size and developmental stage; i.e. younger embryos had uncleared fusion plates and older ones had cleared, so this parameter was not considered. All 18 E12.5 wild type inner ears were normal (Fig. 1S). Virtually all (35/36) heterozygotes showed a reduction in the posterior semicircular canal, but we could not clearly distinguish reduction from complete absence (Fig. 1T), and all 13 homozygotes had a reduced/absent posterior canal and a shortened cochlear duct (Fig. 1U). Therefore, *Fgf10* is required for normal vestibular and cochlear development before E12.5.

At E11.5, a stage at which no embryonic inner ears showed canal pouch fusion plate clearing, only two morphologic classes were evident. All 26 wild type and all 38 heterozygous embryos had a normal morphology (Fig. 1V, W) and all 14 homozygotes appeared narrower than normal along the anterior-posterior axis and had a cochlear duct that had not initiated coiling (Fig. 1X). Therefore, *Fgf10* heterozygosity has its first effect on vestibular morphogenesis between E11.5 and E12.5, whereas the complete absence of *Fgf10* affects both vestibular and cochlear morphogenesis as early as E11.5. We did not attempt to paint-fill E10.5 intercross inner ears, but histologic studies of a limited number of samples did not reveal obvious differences between genotypes (Suppl. Fig. 1). Since the *Fgf10* null vestibular phenotype has been well documented (Ohuchi et al., 2005; Pauley et al., 2003), but the cochlear phenotype is relatively unexplored, we focused subsequent studies on the cochlea.

Fgf10 is required for development of two discrete regions of non-sensory cochlear epithelial tissue

To determine whether the abnormal cochlear morphogenesis observed in *Fgf10*$^{-/-}$ inner ears was accompanied by any cellular changes, we compared hematoxylin and eosin-stained histologic sections of *Fgf10*$^{-/-}$ cochlear ducts with those from *Fgf10*$^{-/+}$ and *Fgf10*$^{+/+}$ embryos. As anticipated from the observations of E15.5 paint-filled inner ears, sagittal sections taken through E18.5 *Fgf10*$^{+/+}$ and *Fgf10*$^{-/+}$ cochleae revealed a normal auditory structure with four cross sections of the cochlear duct visible (Fig. 2A, B), whereas *Fgf10*$^{-/-}$ cochleae were shorter and less extensively coiled, with only three cross sections of the cochlear duct evident (Fig. 2C). We were surprised to find that the *Fgf10* null cochlear duct (scala media, m) was not simply shorter, but also had a significantly reduced cross-sectional area. In the basal turn, the cross sectional area of the mutant scala media averaged only 17.6% of the corresponding wild type or heterozygous area ($n = 3$; $P < 0.0009$), whereas there was no significant difference between mutants and controls with respect to the cross sectional area of the basal scala tympani (t) or scala vestibuli (v) (Fig. 2D). Furthermore, compared to wild type and heterozygous cochlear ducts (Fig. 2A', B'), *Fgf10*$^{-/-}$ cochlear ducts appeared to lack Reissner's membrane (Rm) and much of the outer sulcus (os) (Fig. 2C'). The *Fgf10*$^{-/-}$ samples appeared to have a normally developed sensory organ of Corti (oC), as well as the non-sensory Kolliker's organ/inner sulcus (Ko), stria vascularis (sv) and spiral ganglion (sg) (Fig. 2A'-C'). Higher magnification views confirmed the normal morphologic appearance and number of inner (+) and outer (*) hair cells, as well as a full complement of the organ of Corti supporting cells in all samples (Fig. 2A"-C").

Molecular markers of Reissner's membrane and the outer sulcus are missing or reduced in Fgf10 null cochleae.

To better characterize the differences between *Fgf10* genotypes at E18.5 we used RNA in situ hybridization or immunostaining of cochlear duct cross sections to detect expression of genes and proteins characteristic of the various cell types. Among these markers was *Fgf10* itself, as the transcript produced by the mutant allele (a deletion of exon 2 that causes a frameshift) is stable (Urness et al., 2011). Consistent with the histologic study, no differences between genotypes were detected using markers of Kolliker's organ (*Fgf10*, *Jag1* and *Tecta*; Fig. 3A-F, O-P), hair cells (*Myo6*; Fig. 3J-L), organ of Corti supporting cells (*Jag1*, *Lfng*, $p27^{Kip}$ and *Tecta*; Fig. 3D-I, M-P), and the intermediate and basal cell layers of the stria vascularis (*Trp2* and *Cldn11*, respectively; Fig. 3Q-T). Because we observed no differences in cochlear histology or marker gene expression between $Fgf10^{+/+}$ and $Fgf10^{+/-}$ samples, we used these genotypes interchangeably as controls in subsequent analyses.

In contrast to the results with Kolliker's organ, organ of Corti and stria vascularis markers, markers of Reissner's membrane normally expressed in either the epithelial (e) or mesenchymal/mesothelial (m) layers (*Fgf9*, *Cdh23* and *Lmx1a*, and *Aldh1a2* (previously, *Raldh2*), respectively) were absent from *Fgf10* null cochleae (Fig. 4A-H). In addition, markers of the outer sulcus (*Lmx1a*, *Bmp4*, *Fgfr2*, *Slc26a4* and *Lgr5*) showed a reduced domain in these mutants (Fig. 4E, F, I-P). However, *Lmx1a* and *Aldh1a2* expression in the stria vascularis was preserved (Fig. 4E-H) similarly to *Trp2* and *Cldn11* at E18.5 (Fig. 3Q-T), further suggesting that this tissue was unaffected by the absence of FGF10. Also, *Cdh23* expression in Kolliker's organ and hair cells (Figs. 4C, D), and *Lgr5* expression in Kolliker's organ (Figs. 4O, P) were retained in *Fgf10* null cochleae, confirming that these cells developed normally.

UU IR Author Manuscript

To further delineate the status of the *Fgf10* null outer sulcus in relation to the organ of Corti, we used combinations of antibodies. MYO7A antibodies label hair cell soma and SOX2 antibodies label nuclei in the lateral half of Kolliker's organ and all organ of Corti supporting cells laterally, including Hensen's cells (Hume et al., 2007). Consistent with all previous markers, these two markers revealed no differences between *Fgf10* genotypes (Fig. 4Q, R). CD44 antibodies label cell surfaces in lateral Kolliker's organ, the outer pillar cell, Claudius cells in the outer sulcus, Reissner's membrane and the stria vascularis (Hertzano et al., 2010), whereas S100A1 antibodies label the soma of the inner hair cell and all supporting cells except pillar cells (Sage et al., 2005) and $p75^{NTR}$ antibodies label the inner pillar cells (Mansour et al., 2013; Mueller et al., 2002). There were no differences between genotypes with respect to S100A1 or $p75^{NTR}$ staining (Fig. 4S-V, green), again showing that *Fgf10* is not uniquely required for organ of Corti supporting cell development. However, CD44 staining differed markedly between genotypes. In *Fgf10* null mutants, the Reissner's membrane domain was absent, as was the lateral domain of the outer sulcus, with only a few of the most medial Claudius cells remaining (Fig. 4S-T, S'-T' red). In contrast, outer pillar cell and stria vascularis staining were preserved. Taken together, the histologic and marker analyses performed at E18.5 show that *Fgf10* null cochleae are missing two non-contiguous, non-sensory regions of the epithelium, namely, Reissner's membrane and most of the outer sulcus.

The requirement for Fgf10 in Reissner's membrane development precedes that in outer sulcus development.

To determine the ontogeny of the cellular defects found in E18.5 *Fgf10* null cochleae and their relation to FGF signaling disruptions, we examined the expression of genes for relevant cell

UU IR Author Manuscript

type-specific markers, as well as FGF signaling components and signaling indicators at progressively younger stages. At E15.5, markers of the presumptive Reissner's membrane, *Cdh23* and *Fgf9* (Pirvola et al., 2004; Wilson et al., 2001), were absent in *Fgf10*$^{-/-}$ samples (Fig. 5A-D). *Aldh1a2* is a marker of both the presumptive Reissner's membrane region and the stria vascularis (Burton et al., 2004; Romand et al., 2001; Romand et al., 2004), and only the former domain was missing from *Fgf10* mutants (Fig. 5E, F). The outer sulcus markers, *Bmp4* and *Lmx1a* (Koo et al., 2009; Morsli et al., 1998) were present in mutants, but had a reduced domain (Fig. 5G-J). At this stage and as noted by others (Pauley et al., 2003), *Fgf10* transcripts were expressed in the prosensory domain of the cochlear epithelium and in the spiral ganglion. As expected, the stable transcripts produced from the *Fgf10* exon 2 deletion allele had a similar distribution in the mutants (Fig. 5K, L). *Fgf3*, which is often redundant with *Fgf10*, is expressed just laterally of *Fgf10* at the edge of the prosensory and outer sulcus domains, but we found no changes in its expression in *Fgf10* mutants (Fig. S2A, B), suggesting that this region is intact.

FGF10 and FGF3 signal mainly through FGFR2b, which is the primary FGFR2 isoform expressed in otic epithelium (Pirvola et al., 2000). Therefore, we used a pan probe that detects all *Fgfr2* transcripts, as a proxy for an *Fgfr2b*-specific probe. As expected (Hayashi et al., 2010; Pirvola et al., 2000), this probe labeled the entire non-sensory domain of the control otic epithelium, including the prospective Reissner's membrane, stria vascularis and outer sulcus (Fig. 5M). The *Fgfr2* domain was reduced in *Fgf10* mutants and was still confined to the thin, non-sensory region (Fig. 5N). FGF10 can also signal through FGFR1b, which is co-expressed with FGFR1c in the otic epithelium (Mansour et al., 2013; Pirvola et al., 2002), and as expected (Hayashi et al., 2010; Pirvola et al., 2002), a pan probe for all *Fgfr1* transcripts detected broad

UU IR Author Manuscript

expression throughout the cochlear epithelium, with a focus just medial to the outer sulcus. This domain was still present in *Fgf10* null mutants (Fig. 5O, P).

Spry2 is a transcriptional target of FGF signaling through the RAS/MAPK pathway (Minowada et al., 1999) and was detected as expected in a domain spanning the lateral prosensory and medial outer sulcus region (Shim et al., 2005) and also weakly in the prospective Reissner's membrane. The Reissner's membrane domain was absent from mutants and the outer sulcus domain was reduced (Fig. 5Q, R). Several other transcriptional targets of FGF signaling (*Erm*, *Pea3, Spry1* and *Dusp6*) were found in the epithelium or surrounding mesenchyme, but none of these was affected in the *Fgf10* mutants (Suppl. Fig. S2C-X). Together, these results suggest that the blocks to Reissner's membrane and outer sulcus development in *Fgf10* mutants occurred earlier than E15.5.

Examination of a subset of the Reissner's membrane and outer sulcus markers in sections taken through the base of the cochlear duct at even earlier stages (E13.5 and E12.5) revealed stage-specific differences. As previously observed (Pirvola et al., 2004), the prospective Reissner's membrane marker, *Fgf9*, had a broad expression domain encompassing most of the thin, non-sensory cochlear epithelium in E12.5 and E13.5 controls (Fig. 6A, K). This domain was substantially reduced, but not completely eliminated in stage-matched *Fgf10* mutants (Fig. 6B, L). In contrast, the prospective outer sulcus marker, *Bmp4*, had the same expression domain in controls and mutants at both stages (Fig. 6C, D, M, N). At these stages and as previously noted by Pirvola et al. (2000), *Fgf10* was expressed in the control prosensory regions (Fig. 6E, O) in a pattern almost exactly complementary to that of *Fgfr2* in the non-sensory tissue (Fig. 6G, Q). As expected, the *Fgf10* expression domain (reflecting perdurant exon 2 deletion transcripts) was unchanged in *Fgf10* mutants (Fig. 6F, P), but at E12.5, the *Fgfr2* domain in the roof of the

UU IR Author Manuscript

mutant duct was reduced (Fig. 6H) relative to the control (Fig. 6G). No further change in *Fgfr2* expression was observed at E13.5 (Fig. 6Q, R). The FGF signaling indicator, *Spry1*, did not overlap with *Fgfr2*, so presumably reveals signaling through FGFR1, which is widely expressed at these stages (Hayashi et al., 2010; Pirvola et al., 2002). The lateral extent of *Spry1* expression was significantly reduced in *Fgf10* mutants at both E13.5 (Fig. 6I, J) and E12.5 (Fig. 6S, T). *Spry2*, which marks the lateral prosensory and medial outer sulcus domains, was unchanged at this stage (Fig. S2U, V). Finally, *Fgf9*, *Fgfr2* and *Spry1* were unaffected at E11.5 (data not shown). Collectively, these data suggest that the specification of Reissner's membrane occurs relatively early in cochlear development, at or before E12.5, while medial outer sulcus specification follows between E13.5 and E15.5.

To determine when the non-sensory tissue deletions affected the overall cochlear duct area, we compared control and mutant cochlear ducts at E12.5, E13.5 and E15.5. Although the mutant means were always less than control means, the difference did not reach significance until E15.5 (Fig. 6U).

Proliferation and death of cochlear epithelial cells are unaffected in *Fgf10* null mutants

To determine whether *Fgf10* is necessary for proliferation of the non-sensory epithelial regions at the stages when they are first developing, we labeled M-phase cells at E11.5 and S-phase cells at E13.5 with antibodies directed against phospho-Histone H3 and pulse-incorporated BrdU, respectively. Samples were co-stained with antibodies directed against SOX2 to distinguish prosensory (SOX2+) from non-sensory (SOX2-) domains (Fig. 7A-D). We determined the average number of proliferation marker-positive cells per unit area in each of the two epithelial domains, but no significant differences between genotypes were evident in either

UU IR Author Manuscript

domain at either stage (Fig. 7E, F). A limited number of E12.5 and E14.5 BrdU-labeled samples was examined and these also showed no evidence of differences between genotypes (data not shown). Similarly, labeling of dying cells at E13.5 with antibodies directed against cleaved Caspase 3 failed to reveal differences between genotypes in either the SOX2+ or SOX2- domain (Fig. 7G, H; n = 3 each); however, the very small number of dying cells, in both control and mutant epithelia, precluded detailed quantitation. Thus, neither proliferation nor cell survival in the non-sensory regions appear to require *Fgf10*.

Discussion

Fgf10 is expressed robustly in the developing inner ear epithelium and ganglion, and has known roles in vestibular morphogenesis. To determine its roles in cochlear development we studied global null mutants and found that in addition to the previously described defects of vestibular morphogenesis in homozygous null mutants (Ohuchi et al., 2005; Pauley et al., 2003), the heterozygotes showed a fully penetrant reduction or loss of the posterior semicircular canal, indicating that this region of the otic labyrinth is particularly sensitive to FGF10 dosage. We also found that while some *Fgf10* null mutants had defects of semicircular canal formation similar to those described previously (Ohuchi et al., 2005; Pauley et al., 2003), others had a more severe defect in which canal fusion plates failed to clear. Most significantly, and the focus of this report, we found that homozygous null mutants had a previously undetected cochlear defect, namely loss or reduction of two non-contiguous non-sensory domains, Reissner's membrane and the outer sulcus, respectively (Fig. 8). This was accompanied by a noticeable shortening of the cochlear duct.

UU IR Author Manuscript

These new cochlear data suggest an interesting parallel between the function of *Fgf10* in the vestibular compartment and its action in the cochlea. *Fgf10* is expressed in the developing semicircular canal prosensory domain (giving rise to the cristae) while *Fgfr2b* is expressed in the non-sensory canal epithelium. Loss of *Fgf10* or chemical blockage of FGF signaling results in the non-sensory canal defects shown here and previously by others (Chang et al., 2004; Ohuchi et al., 2005; Pauley et al., 2003). Similarly, *Fgf10* is expressed in a sensory-competent domain early in cochlear development, eventually becoming restricted in mice to lateral Kolliker's organ, adjacent to the organ of Corti (Ohyama et al., 2010; Pujades et al., 2006; Sanchez-Guardado et al., 2013), and, as we have shown here, is required for specification of two non-sensory domains expressing *Fgfr2b*. Thus, in contrast to the epithelial-mesenchymal signaling paradigm apparent in other FGF10-dependent structures (Beenken and Mohammadi, 2009; Itoh and Ornitz, 2011; Turner and Grose, 2010), non-sensory development in the inner ear may depend upon intraepithelial paracrine signaling as posited by Pirvola et al. (2000).

When and how do the *Fgf10* cochlear phenotypes arise? Analysis of numerous cell type specific markers showed that the two affected non-sensory tissues appear to initiate development at different times when *Fgf10* and *Fgfr2b* are expressed in adjacent cochlear epithelial domains, with the medial Reissner's membrane initiating first at E12.5-13.5, and the lateral outer sulcus domain initiating later at E15.5 (Fig. 8). The failure to generate these two non-sensory tissues did not appear to be compensated for by expansion of other tissues, and by E15.5, the mutant cochlear duct area was significantly less than that of controls. The lack of an effect on proliferation or cell death at the two boundaries of the *Fgf10* and *Fgfr2b* expression domains suggests that both phenotypes are likely to result from defects of localized progenitor cell specification rather than a failure of proliferation or cell survival.

UU IR Author Manuscript

Fgf10 and Reissner's membrane

The molecular mechanisms by which FGF10 induces Reissner's membrane and outer sulcus development are not clear, but our data suggest some possibilities that could be tested in future studies. Reissner's membrane spans the region between Kolliker's organ and the stria vascularis. It consists of an inner, epithelial layer facing the endolymph of the scala media and an outer mesothelial layer facing the perilymph of the scala vestibuli. Its function is to help maintain the distinct ionic compositions of endolymph and perilymph (Kim et al., 2014; Kim and Marcus, 2011) as well as to propagate traveling waves that play a role in otoacoustic emissions (Reichenbach et al., 2012). The genetic networks required for Reissner's membrane development are unexplored. Ours is the first report detailing the specific and complete loss Reissner's membrane via mutation of a gene expressed locally within the cochlear epithelium. Given the dramatic reduction of *Fgf9* found in the presumptive Reissner's membrane of *Fgf10* null mutants at E12.5-E13.5, it is tempting to speculate that *Fgf9* functions downstream of *Fgf10* in specification of Reissner's membrane. However, *Fgf9* null mutants retain Reissner's membrane, albeit with detachment of the mesothelial and epithelial layers. In addition, *Fgf9* mutants exhibit other dysmorphic features of the scala vestibuli (enlargement and irregular trabeculae) and they have a normally proportioned and elongated cochlea (Pirvola et al., 2004). None of these features are recapitulated in *Fgf10* mutants. Thus, the down-regulation of *Fgf9* in the *Fgf10* null cochleae may be more correlative than causal, and low-level expression of *Fgf9* at E12.5-13.5 in *Fgf10* mutants may be sufficient to provide its normal function in signaling to the mesenchyme.

Aldh1a2, encoding a retinoic acid biosynthetic enzyme, is strongly expressed in the mesenchymal/mesothelial domain of Reissner's membrane at E18.5 and was absent in *Fgf10*

mutants, but we did not observe any expression in or adjacent to the cochlear duct at E12.5-E13.5, when Reissner's membrane is induced. Thus it is unlikely to play a role downstream of *Fgf10* in its specification. Nevertheless, the later mesechymal/mesothelial expression of *Aldh1a2* remains suggestive of a role in Reissner's membrane development, possibly in conjunction with epithelial *Fgf9*. Addressing this issue will require analysis of appropriate conditional mutants.

Lmx1a, which encodes a LIM homeodomain-containing transcription factor and is expressed in the prospective and late embryonic epithelial Reissner's membrane of controls, but was absent from *Fgf10* null mutants, may be a more likely candidate as a downstream effector of FGF10 signaling in Reissner's membrane specification. *Lmx1a* likely null mutants (*dreher, mtl, bsd*) have dysmorphic cochleae in which the basal sensory domain is merged with and resembles a neighboring vestibular sensory domain (Koo et al., 2009; Nichols et al., 2008; Steffes et al., 2012), suggesting improper sensory boundary formation. This phenotype is not seen in *Fgf10* null mutants. However, Reissner's membrane appears abnormal in *Lmx1a* mutants, with a possible reduction in the cross sectional area of the cochlear duct (Nichols et al., 2008), and further examination and comparison with *Fgf10* null mutants is warranted. In addition, as in *Fgf10* null mutants, the *Lmx1a* mutant cochleae are shortened (Koo et al., 2009; Nichols et al., 2008; Steffes et al., 2012). As *Fgf10* transcripts are not affected in the *Lmx1a* cochlea (Nichols et al., 2008), but the Reissner's membrane and outer sulcus domains of *Lmx1a* transcripts are absent from *Fgf10* null mutants (this study), it is likely that *Fgf10* is upstream of *Lmx1a.* Whether *Lmx1a* actually mediates FGF10 functions in the cochlear duct could only be tested by replacing its function in the *Fgf10* null mutant.

Fgf10 and the outer sulcus

UU IR Author Manuscript

Similar to the role of Reissner's membrane, the outer sulcus provides a crucial component of the non-sensory epithelial compartment of the cochlear duct. Cells in this domain actively reabsorb cations from the endolymph, providing the optimum homeostatic environment for mechanoelectrical transduction to occur in hair cells (Jagger and Forge, 2013; Kim and Marcus, 2011). As with Reissner's membrane, we do not yet have a clear grasp on the regulatory pathways by which *Fgf10* orchestrates outer sulcus development, but it is reasonable to suggest that *Fgf10* may do so by regulating expression of *Bmp4.* Conditional mutagenesis of *Alk3* and *Alk6,* encoding type I BMP receptors, revealed that BMP signaling, like *Fgf10* signaling, is required for outer sulcus specification and normal cochlear length. The *Alk* mutants exhibit a lateral expansion of the cochlear *Fgf10* expression domain in Kolliker's organ at E13.5. Furthermore, exposure of cochlear organ cultures to BMP4 ligand induces markers of the outer sulcus and suppresses *Fgf10* and other markers of Kolliker's organ, suggesting that BMP signaling negatively regulates FGF signaling in the cochlear duct. (Ohyama et al., 2010). Our data suggest that FGF10 may be a positive regulator of *Bmp4* expression, but since there is residual *Bmp4* expression and residual outer sulcus tissue in *Fgf10* mutants and other BMP ligands may also be present in either the epithelium or mesenchyme, it is not surprising that we did not observe an expansion of the $Fgf10^{\Delta 2}$ expression domain in mutants. Further studies will be required to dissect the regulatory relationships between FGF and BMP signaling in cochlear duct patterning and morphogenesis. In addition, it will be interesting to learn whether removing the remaining FGFR2b ligand (FGF3) leads to complete deletion of the outer sulcus.

Fgf10 and cochlear length

UU IR Author Manuscript

Despite the obvious, but relatively mild, shortening of the cochlear duct noted in gross observations of *Fgf10* null mutants, we did not detect proliferative differences that could account for this phenotype. Additional studies may be necessary to determine if the shortening is in fact caused by small effects on proliferation or instead by an alternative mechanism, such as a slowing of convergent extension (McKenzie et al., 2004; Yamamoto et al., 2009). Indeed, the cells in the residual *Bmp4*-positive outer sulcus region of the mutants appear taller than those of control cochleae. As reducing the dosage of *Fgf3*, which encodes a ligand with the same receptor activating profile as FGF10 (Zhang et al., 2006), leads to further shortening of the *Fgf10* null cochlea (data not shown, manuscript in preparation), and *Fgfr2b* null mutants never develop a cochlea (Pirvola et al., 2000), we suspect that FGF10 together with FGF3-stimulated proliferation will prove to be one of the factors regulating cochlear length.

Implications for human hearing loss

Heterozygous mutations in FGF10 leading to reduced signaling activity are a cause of the very rare autosomal dominant LADD (lacrimo-auriculo-dento-digital) syndrome and its allelic variant, ASLG (aplasia of lacrimal and salivary glands) syndrome. LADD syndrome is also caused by heterozygous mutations in FGFR2 and FGFR3 that reduce signaling activity (Milunsky et al., 2006; Rohmann et al., 2006; Shams et al., 2007). Neither LADD nor ASLG subjects, nor mice that are heterozygous for *Fgf10, Fgfr2* or *Fgfr3* loss-of-function mutations have ever been reported with vestibular symptoms. In light of our findings that $Fgf10^{-/+}$ mice have posterior semicircular canal defects, it would be interesting to image the inner ears of LADD subjects with known *FGF10* mutations to determine the status of the posterior semicircular canal. Interestingly, there is a case report of a LADD syndrome subject with

UU IR Author Manuscript

unilateral dysplastic posterior and lateral semicircular canals (Moses, 2013), and another with bilateral dysplasia of the semicircular canals (Azar et al., 2000), but no information about the responsible mutations is available. Given that only one semicircular canal is affected in mice, it is likely that the remainder of the vestibular system compensates, though it is possible that an abnormal vestibular phenotype might be revealed with specific testing.

55% of LADD syndrome subjects are reported with hearing loss (Milunsky et al., 2006), but the type (conductive, sensorineural or mixed) is not always specified and the mutation status is rarely known. Nevertheless, imaging of some of these individuals has revealed cochlear hypoplasia (Lemmerling et al., 1999; Meuschel-Wehner et al., 2002; Moses, 2013). We did not detect any morphologic or molecular aberrations in the cochlear ducts of *Fgf10* heterozygotes and their hearing is normal (Mansour et al., 2013), but homozygotes had cochlear defects that would be expected to cause hearing loss if the other major consequences of *Fgf10* homozygosity, such as the failure of lung development, could be bypassed. In particular, the failure of normal Reissner's membrane and outer sulcus development, both of which are important in maintaining the endolymph homeostasis necessary for hearing, suggests that these tissues could be compromised to some extent even in LADD syndrome subjects without reported cochlear malformations and might contribute to the hearing loss reported in some individuals. Our inner ear findings in mice suggest that LADD and ASLG syndrome subjects should receive hearing and vestibular function evaluations and counseling as part of their clinical care.

In summary, our findings on the development of *Fgf10* null inner ears provide new insight into the specification of cochlear non-sensory domains and suggest a basis for the hearing loss reported for some LADD syndrome subjects.

UU IR Author Manuscript

Acknowledgements

We are grateful to the numerous colleagues who supplied the DNA clones used to prepare probes for ISH; they are acknowledged in Supplementary Table 1. We thank Jerry Spangrude for rat anti-CD44, Tim Goodman for advice regarding BrdU detection, Shannon Odelberg for consultations regarding statistical analyses and Gary Schoenwolf for helpful comments on the manuscript. This work was supported by grants to S.L.M from the NIDCD/NIH (DC011819) and to T.O. from NIDCD/NIH (DC012085). These funding sources had no involvement in the study design, data collection, analysis or interpretation, or in the writing or choice of where to submit this report.

UU IR Author Manuscript

References

Alvarez, Y., Alonso, M. T., Vendrell, V., Zelarayan, L. C., Chamero, P., Theil, T., Bosl, M. R., Kato, S., Maconochie, M., Riethmacher, D., Schimmang, T., 2003. Requirements for FGF3 and FGF10 during inner ear formation. Development. 130**,** 6329-6338.

Azar, T., Scott, J. A., Arnold, J. E., Robin, N. H., 2000. Epiglottic hypoplasia associated with lacrimo-auriculo-dental-digital syndrome. Ann Otol Rhinol Laryngol. 109**,** 779-781.

Beenken, A., Mohammadi, M., 2009. The FGF family: biology, pathophysiology and therapy. Nat Rev Drug Discov. 8**,** 235-253.

Burton, Q., Cole, L. K., Mulheisen, M., Chang, W., Wu, D. K., 2004. The role of Pax2 in mouse inner ear development. Dev Biol. 272**,** 161-175.

Chang, W., Brigande, J. V., Fekete, D. M., Wu, D. K., 2004. The development of semicircular canals in the inner ear: role of FGFs in sensory cristae. Development. 131**,** 4201-4211.

Groves, A. K., Fekete, D. M., 2012. Shaping sound in space: the regulation of inner ear patterning. Development. 139**,** 245-257.

Hatch, E. P., Noyes, C. A., Wang, X., Wright, T. J., Mansour, S. L., 2007. *Fgf3* is required for dorsal patterning and morphogenesis of the inner ear epithelium. Development. 134**,** 3615-3625.

Hayashi, T., Ray, C. A., Younkins, C., Bermingham-McDonogh, O., 2010. Expression patterns of FGF receptors in the developing mammalian cochlea. Dev Dyn. 239**,** 1019-1026.

Hertzano, R., Puligilla, C., Chan, S. L., Timothy, C., Depireux, D. A., Ahmed, Z., Wolf, J., Eisenman, D. J., Friedman, T. B., Riazuddin, S., Kelley, M. W., Strome, S. E., 2010. CD44 is a marker for the outer pillar cells in the early postnatal mouse inner ear. J Assoc Res Otolaryngol. 11**,** 407-418.

Hume, C. R., Bratt, D. L., Oesterle, E. C., 2007. Expression of LHX3 and SOX2 during mouse inner ear development. Gene Expr Patterns. 7**,** 798-807.

Hurley, P. A., Clarke, M., Crook, J. M., Wise, A. K., Shepherd, R. K., 2003. Cochlear immunochemistry--a new technique based on gelatin embedding. J Neurosci Methods. 129**,** 81-86.

Itoh, N., Ornitz, D. M., 2011. Fibroblast growth factors: from molecular evolution to roles in development, metabolism and disease. J Biochem. 149**,** 121-130.

Jagger, D. J., Forge, A., 2013. The enigmatic root cell - emerging roles contributing to fluid homeostasis within the cochlear outer sulcus. Hear Res. 303**,** 1-11.

Kiernan, A. E., 2006. The paintfill method as a tool for analyzing the three-dimensional structure of the inner ear. Brain Res. 1091**,** 270-276.

Kim, K. X., Sanneman, J. D., Kim, H. M., Harbidge, D. G., Xu, J., Soleimani, M., Wangemann, P., Marcus, D. C., 2014. Slc26a7 chloride channel activity and localization in mouse Reissner's membrane epithelium. PLoS One. 9**,** e97191.

Kim, S. H., Marcus, D. C., 2011. Regulation of sodium transport in the inner ear. Hear Res. 280**,** 21-29.

Koo, S. K., Hill, J. K., Hwang, C. H., Lin, Z. S., Millen, K. J., Wu, D. K., 2009. Lmx1a maintains proper neurogenic, sensory, and non-sensory domains in the mammalian inner ear. Dev Biol. 333**,** 14-25.

Ladher, R. K., Wright, T. J., Moon, A. M., Mansour, S. L., Schoenwolf, G. C., 2005. FGF8 initiates inner ear induction in chick and mouse. Genes Dev. 19**,** 603-613.

UU IR Author Manuscript

Lemmerling, M. M., Vanzieleghem, B. D., Dhooge, I. J., Van Cauwenberge, P. B., Kunnen, M. F., 1999. The Lacrimo-Auriculo-Dento-Digital (LADD) syndrome: temporal bone CT findings. J Comput Assist Tomogr. 23**,** 362-364.

Mafong, D. D., Shin, E. J., Lalwani, A. K., 2002. Use of laboratory evaluation and radiologic imaging in the diagnostic evaluation of children with sensorineural hearing loss. Laryngoscope. 112**,** 1-7.

Mansour, S. L., Goddard, J. M., Capecchi, M. R., 1993. Mice homozygous for a targeted disruption of the proto-oncogene *int-2* have developmental defects in the tail and inner ear. Development. 117**,** 13-28.

Mansour, S. L., Li, C., Urness, L. D., 2013. Genetic rescue of Muenke syndrome model hearing loss reveals prolonged FGF-dependent plasticity in cochlear supporting cell fates. Genes Dev. 27**,** 2320-2331.

McKenzie, E., Krupin, A., Kelley, M. W., 2004. Cellular growth and rearrangement during the development of the mammalian organ of Corti. Dev Dyn. 229**,** 802-812.

Meuschel-Wehner, S., Klingebiel, R., Werbs, M., 2002. Inner ear dysplasia in sporadic lacrimo-auriculo-dento-digital syndrome. A case report and review of the literature. ORL J Otorhinolaryngol Relat Spec. 64**,** 352-354.

Milunsky, J. M., Zhao, G., Maher, T. A., Colby, R., Everman, D. B., 2006. LADD syndrome is caused by FGF10 mutations. Clin Genet. 69**,** 349-354.

Minowada, G., Jarvis, L. A., Chi, C. L., Neubuser, A., Sun, X., Hacohen, N., Krasnow, M. A., Martin, G. R., 1999. Vertebrate Sprouty genes are induced by FGF signaling and can cause chondrodysplasia when overexpressed. Development. 126**,** 4465-4475.

Morsli, H., Choo, D., Ryan, A., Johnson, R., Wu, D. K., 1998. Development of the mouse inner ear and origin of its sensory organs. J Neurosci. 18**,** 3327-3335.

Moses, J. E., 2013. Lacrimo-auriculo-dento-digital syndrome with unilateral inner ear dysplasia and craniocervical osseous abnormalities: case report and review of literature. Clin Neuroradiol. 23**,** 221-224.

Mueller, K. L., Jacques, B. E., Kelley, M. W., 2002. Fibroblast growth factor signaling regulates pillar cell development in the organ of corti. J Neurosci. 22**,** 9368-9377.

Nichols, D. H., Pauley, S., Jahan, I., Beisel, K. W., Millen, K. J., Fritzsch, B., 2008. Lmx1a is required for segregation of sensory epithelia and normal ear histogenesis and morphogenesis. Cell Tissue Res. 334**,** 339-358.

Ohuchi, H., Yasue, A., Ono, K., Sasaoka, S., Tomonari, S., Takagi, A., Itakura, M., Moriyama, K., Noji, S., Nohno, T., 2005. Identification of *cis*-element regulating expression of the mouse *Fgf10* gene during inner ear development. Dev Dyn. 233**,** 177-187.

Ohyama, T., Basch, M. L., Mishina, Y., Lyons, K. M., Segil, N., Groves, A. K., 2010. BMP signaling is necessary for patterning the sensory and nonsensory regions of the developing mammalian cochlea. J Neurosci. 30**,** 15044-15051.

Pauley, S., Wright, T. J., Pirvola, U., Ornitz, D., Beisel, K., Fritzsch, B., 2003. Expression and function of FGF10 in mammalian inner ear development. Dev Dyn. 227**,** 203-215.

Pirvola, U., Spencer-Dene, B., Xing-Qun, L., Kettunen, P., Thesleff, I., Fritzsch, B., Dickson, C., Ylikoski, J., 2000. FGF/FGFR-2(IIIb) signaling is essential for inner ear morphogenesis. J Neurosci. 20**,** 6125-6134.

Pirvola, U., Ylikoski, J., Trokovic, R., Hebert, J. M., McConnell, S. K., Partanen, J., 2002. FGFR1 is required for the development of the auditory sensory epithelium. Neuron. 35**,** 671-680.

UU IR Author Manuscript

Pirvola, U., Zhang, X., Mantela, J., Ornitz, D. M., Ylikoski, J., 2004. *Fgf9* signaling regulates inner ear morphogenesis through epithelial-mesenchymal interactions. Dev Biol. 273**,** 350-360.

Pujades, C., Kamaid, A., Alsina, B., Giraldez, F., 2006. BMP-signaling regulates the generation of hair-cells. Dev Biol. 292**,** 55-67.

Reichenbach, T., Stefanovic, A., Nin, F., Hudspeth, A. J., 2012. Waves on Reissner's membrane: a mechanism for the propagation of otoacoustic emissions from the cochlea. Cell Rep. 1**,** 374-384.

Rohmann, E., Brunner, H. G., Kayserili, H., Uyguner, O., Nurnberg, G., Lew, E. D., Dobbie, A., Eswarakumar, V. P., Uzumcu, A., Ulubil-Emeroglu, M., Leroy, J. G., Li, Y., Becker, C., Lehnerdt, K., Cremers, C. W., Yuksel-Apak, M., Nurnberg, P., Kubisch, C., Schlessinger, J., van Bokhoven, H., Wollnik, B., 2006. Mutations in different components of FGF signaling in LADD syndrome. Nat Genet. 38**,** 414-417.

Romand, R., Albuisson, E., Niederreither, K., Fraulob, V., Chambon, P., Dolle, P., 2001. Specific expression of the retinoic acid-synthesizing enzyme RALDH2 during mouse inner ear development. Mech Dev. 106**,** 185-189.

Romand, R., Niederreither, K., Abu-Abed, S., Petkovich, M., Fraulob, V., Hashino, E., Dolle, P., 2004. Complementary expression patterns of retinoid acid-synthesizing and -metabolizing enzymes in pre-natal mouse inner ear structures. Gene Expr Patterns. 4**,** 123-133.

Sage, C., Huang, M., Karimi, K., Gutierrez, G., Vollrath, M. A., Zhang, D. S., Garcia-Anoveros, J., Hinds, P. W., Corwin, J. T., Corey, D. P., Chen, Z. Y., 2005. Proliferation of functional hair cells in vivo in the absence of the retinoblastoma protein. Science. 307**,** 1114-1118.

Sanchez-Guardado, L. O., Puelles, L., Hidalgo-Sanchez, M., 2013. Fgf10 expression patterns in the developing chick inner ear. J Comp Neurol. 521**,** 1136-1164.

Shams, I., Rohmann, E., Eswarakumar, V. P., Lew, E. D., Yuzawa, S., Wollnik, B., Schlessinger, J., Lax, I., 2007. Lacrimo-auriculo-dento-digital syndrome is caused by reduced activity of the fibroblast growth factor 10 (FGF10)-FGF receptor 2 signaling pathway. Mol Cell Biol. 27**,** 6903-6912.

Shim, K., Minowada, G., Coling, D. E., Martin, G. R., 2005. Sprouty2, a mouse deafness gene, regulates cell fate decisions in the auditory sensory epithelium by antagonizing FGF signaling. Dev Cell. 8**,** 553-564.

Steffes, G., Lorente-Canovas, B., Pearson, S., Brooker, R. H., Spiden, S., Kiernan, A. E., Guenet, J. L., Steel, K. P., 2012. Mutanlallemand (mtl) and Belly Spot and Deafness (bsd) are two new mutations of Lmx1a causing severe cochlear and vestibular defects. PLoS One. 7**,** e51065.

Turner, N., Grose, R., 2010. Fibroblast growth factor signalling: from development to cancer. Nat Rev Cancer. 10**,** 116-129.

Urness, L. D., Bleyl, S. B., Wright, T. J., Moon, A. M., Mansour, S. L., 2011. Redundant and dosage sensitive requirements for Fgf3 and Fgf10 in cardiovascular development. Dev Biol. 356**,** 383-397.

Urness, L. D., Li, C., Wang, X., Mansour, S. L., 2008. Expression of ERK signaling inhibitors *Dusp6*, *Dusp7*, and *Dusp9* during mouse ear development. Dev Dyn. 237**,** 163-169.

UU IR Author Manuscript

Urness, L. D., Paxton, C. N., Wang, X., Schoenwolf, G. C., Mansour, S. L., 2010. FGF signaling regulates otic placode induction and refinement by controlling both ectodermal target genes and hindbrain *Wnt8a*. Dev Biol. 340**,** 595-604.

Wilson, S. M., Householder, D. B., Coppola, V., Tessarollo, L., Fritzsch, B., Lee, E. C., Goss, D., Carlson, G. A., Copeland, N. G., Jenkins, N. A., 2001. Mutations in *Cdh23* cause nonsyndromic hearing loss in waltzer mice. Genomics. 74**,** 228-233.

Wright, T. J., Mansour, S. L., 2003. Fgf3 and Fgf10 are required for mouse otic placode induction. Development. 130**,** 3379-3390.

Wu, C. C., Chen, Y. S., Chen, P. J., Hsu, C. J., 2005. Common clinical features of children with enlarged vestibular aqueduct and Mondini dysplasia. Laryngoscope. 115**,** 132-137.

Wu, D. K., Kelley, M. W., 2012. Molecular mechanisms of inner ear development. Cold Spring Harb Perspect Biol. 4**,** a008409.

Yamamoto, N., Okano, T., Ma, X., Adelstein, R. S., Kelley, M. W., 2009. Myosin II regulates extension, growth and patterning in the mammalian cochlear duct. Development. 136**,** 1977-1986.

Zelarayan, L. C., Vendrell, V., Alvarez, Y., Domínguez-Frutos, E., Theil, T., Alonso, M. T., Maconochie, M., Schimmang, T., 2007. Differential requirements for FGF3, FGF8 and FGF10 during inner ear development. Developmental Biology. 308**,** 379-391.

Zhang, X., Ibrahimi, O. A., Olsen, S. K., Umemori, H., Mohammadi, M., Ornitz, D. M., 2006. Receptor specificity of the fibroblast growth factor family. The complete mammalian FGF family. J Biol Chem. 281**,** 15694-15700.

UU IR Author Manuscript

Figure Legends

Figure 1. Vestibular morphogenesis is affected in both *Fgf10* heterozygous and *Fgf10* homozygous null mutants, whereas cochlear development is affected only in homozygotes. (A-E, G-K, M-Q, S-X) Inner ear epithelia were filled with paint at the stages indicated to the left of each row. Genotypes are indicated at the top of each column. The phenotypic class designations for E13.5-E15.5 samples as described in the main text (C0-C4) are summarized in panel Y and indicated in the upper right portion of each panel. The percentage of each E13.5-E15.5 genotype falling into each phenotypic class is shown (F, L, R). Abbreviations: aa, anterior ampula; ascc, anterior semicircular canal; cd, cochlear duct; la, lateral ampula; lscc, lateral semicircular canal; pa, posterior ampula; pscc, posterior semicircular canal; vcp, vertical canal plate.

Figure 2. *Fgf10* null cochlear ducts lack non-sensory domains and have a reduced cross-sectional area. Hematoxylin and eosin-stained E18.5 cochlear duct cross sections at three magnifications. Boxes in A-C indicate the region magnified in A'-C'. Dashed boxes in A'-C'; indicate the region magnified in A"-C". C" Morphologic structures remaining in *Fgf10* mutants are indicated with lines. Genotypes are indicated to the left of each row. D. Graphical comparison of the cross sectional area of basal scalae (n = 3 controls and 3 mutants). Abbreviations: Ko, Kolliker's organ; m, scala media (cochlear duct), oC, organ of Corti; os, outer sulcus; Rm, Reissner's membrane; sg, spiral (cochlear) ganglion; sv, stria vascularis; t, scala tympani; v, scala vestibuli. Asterisks indicate outer hair cells, plus symbols indicate inner hair cells. Scale bars in A, A', A'' apply to all panels in the same column.

UU IR Author Manuscript

Figure 3. Markers of Kolliker's organ, supporting cells, hair cells and the stria vascularis are unchanged in E18.5 *Fgf10* null mutants. In situ hybridization (A-L, O-T) or immunostaining analysis (M, N) of cochlear cross sections. Genotypes are indicated to the left of each row and probes are indicated at the upper right of the top panel in each series. Abbreviations: hc, hair cells; Ko, Kolliker's organ; sc, supporting cells; sv, stria vascularis. Scale bar in A applies to all panels.

Figure 4. Markers of Reissner's membrane are absent and outer sulcus markers show a reduced domain in E18.5 *Fgf10* null mutant cochleae. In situ hybridization (A-P) and immunostaining (Q-V) analyses of basal cochlear duct cross sections. Genotypes are indicated to the left of each row and probes are indicated to the upper right of each pair of panels. Insets in A, C, E, G show magnifications of Reissner's membrane. S'-T' provide enlargements of S-T, with the arrow in T' indicating the remnant Claudius cells in the mutant os. Abbreviations: Rm(e), Reissner's membrane-epithelial layer; Rm(m), Reissner's membrane-mesenchymal/mesothelial domain; os, outer sulcus. See Figure 2 or 3 legend for others. Scale bar in A applies to all panels except S'-T'. Scale bar in S' applies to T'.

Figure 5. Presumptive Reissner's membrane markers are absent and presumptive outer sulcus markers show a reduced domain in E15.5 *Fgf10* null mutant cochleae. In situ hybridization analyses of basal cochlear duct cross sections are shown. Genotypes are indicated to the left of each row and probes are indicated to the upper right of each pair of panels. Dashed and solid lines indicate expression that is altered or unchanged, respectively, in mutants. Abbreviations: Ko, presumptive Kolliker's organ; os, presumptive outer sulcus; ps, presumptive

UU IR Author Manuscript

prosensory domain; Rm, presumptive Reissner's membrane; sg, spiral ganglion; sv, stria vascularis. Scale bar in A applies to all panels.

Figure 6. The effects of FGF10 absence on Reissner's membrane development precede those on outer sulcus development. In situ hybridization analyses of basal cochlear duct cross sections at E13.5 (A-J) and E12.5 (K-T). Genotypes are indicated to the left of each row and probes are indicated to the upper right of the top panels. Dashed and solid black lines indicate expression that is altered or unchanged, respectively, in mutants. The cochlear duct is outlined with a dashed grey line. U. Graphical comparison of the cochlear duct area of the basal scala media at the developmental ages shown (n = 3 controls and 3 mutants). Abbreviations: Ko, Kolliker's organ; Rm, presumptive Reissner's membrane; os, outer sulcus; ps, prosensory region; sg, spiral ganglion; sv, stria vascularis. Scale bar in A applies to all panels.

Figure 7. Neither cell proliferation nor cell survival is altered in *Fgf10* null cochlear ducts. Double labeling of control (A) and *Fgf10* null (B) E11.5 cochlear duct cross sections with antibodies directed against phospho-Histone H3 (red) and SOX2 (green). Nuclei are counterstained with DAPI (blue). Double labeling of control (C) and *Fgf10* null (D) E13.5 cochlear duct cross sections with antibodies directed against BrdU (red) and SOX2 (green). Dotted lines delineate the regions considered non-sensory (SOX2-). The remaining SOX2+ areas were considered prosensory. Graphical comparisons of the mean number of proliferating cells per pixel^2 in SOX2+ (E) and SOX2- (F) regions of control (white bars) and *Fgf10* null mutants (black bars). Error bars indicate standard deviation (SD). Double labeling of control (G) and *Fgf10* null (H) E13.5 cochlear duct cross sections with antibodies directed against cleaved

UU IR Author Manuscript

Caspase 3 (cCasp3; red) and SOX2 (green). Nuclei are counterstained with DAPI (blue). Abbreviation: g, ganglion. Scale bar in panel A applies to all images.

Figure 8. Model depicting the effects of FGF10 absence on development of non-sensory cochlear domains. (A) At E12.5-E13.5 FGF10 induces Reissner's membrane development at the medial boundary of *Fgf10/Fgfr2* expression. (B) By E15.5, FGF10 induces outer sulcus development at the lateral boundary of *Fgf10/Fgfr2* expression. Expression domains of *Fgf10* and receptor genes are color coded in A and B. (C) Failure of FGF10 signaling leads by E18.5 to a total loss of Reissner's membrane and a significant reduction in the outer sulcus. Both affected domains are colored brown. Other morphologic domains are delineated and the now quite separated expression domains for *Fgf10* and *Fgfr2* are indicated with black arcs. There is low-level diffuse expression of *Fgfr1* throughout much of the cochlear duct at all stages (not shown). $Fgf10^{\Delta 2}$ refers to the stable exon 2-deleted transcript that does not encode functional FGF10, but perdures in the mutant. All other abbreviations have been defined previously.

Two Supplementary Tables and two Supplementary Figures, all with legends, are found after the regular Figures (PDF version of manuscript only).

UU IR Author Manuscript

Figure 1

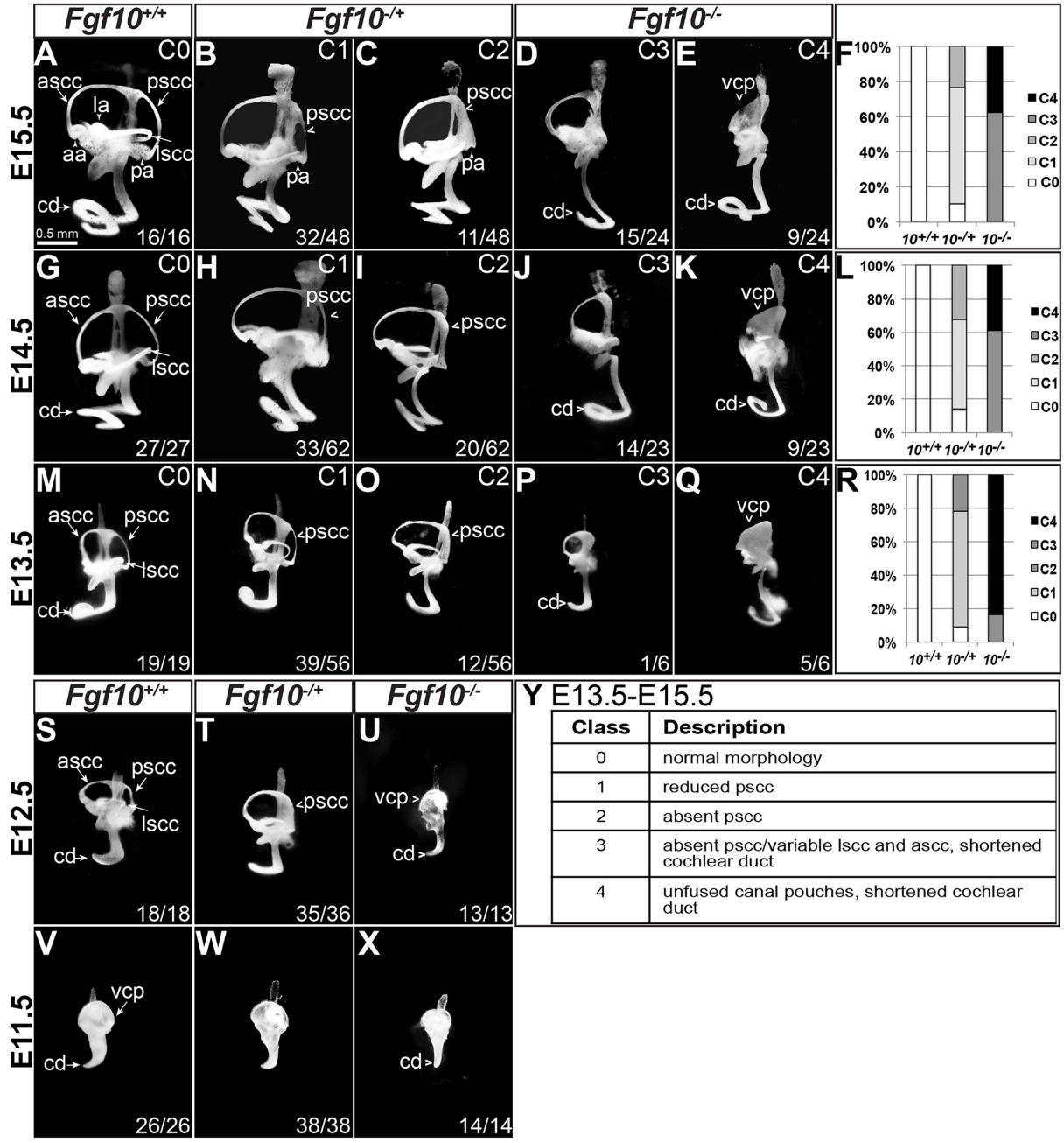

Figure 1. Vestibular morphogenesis is affected in both *Fgf10* heterozygous and *Fgf10* homozygous null mutants, whereas cochlear development is affected only in homozygotes. (A-E, G-K, M-Q, S-X) Inner ear epithelia were filled with paint at the stages indicated to the left of each row. Genotypes are indicated at the top of each column. The phenotypic class designations for E13.5-E15.5 samples as described in the main text (C0-C4) are summarized in panel Y and indicated in the upper right portion of each panel. The percentage of each E13.5-E15.5 genotype falling into each phenotypic class is shown (F, L, R). Abbreviations: aa, anterior ampula; ascc, anterior semicircular canal; cd, cochlear duct; la, lateral ampula; lscc, lateral semicircular canal; pa, posterior ampula; pscc, posterior semicircular canal; vcp, vertical canal plate.

UU IR Author Manuscript

Figure 2

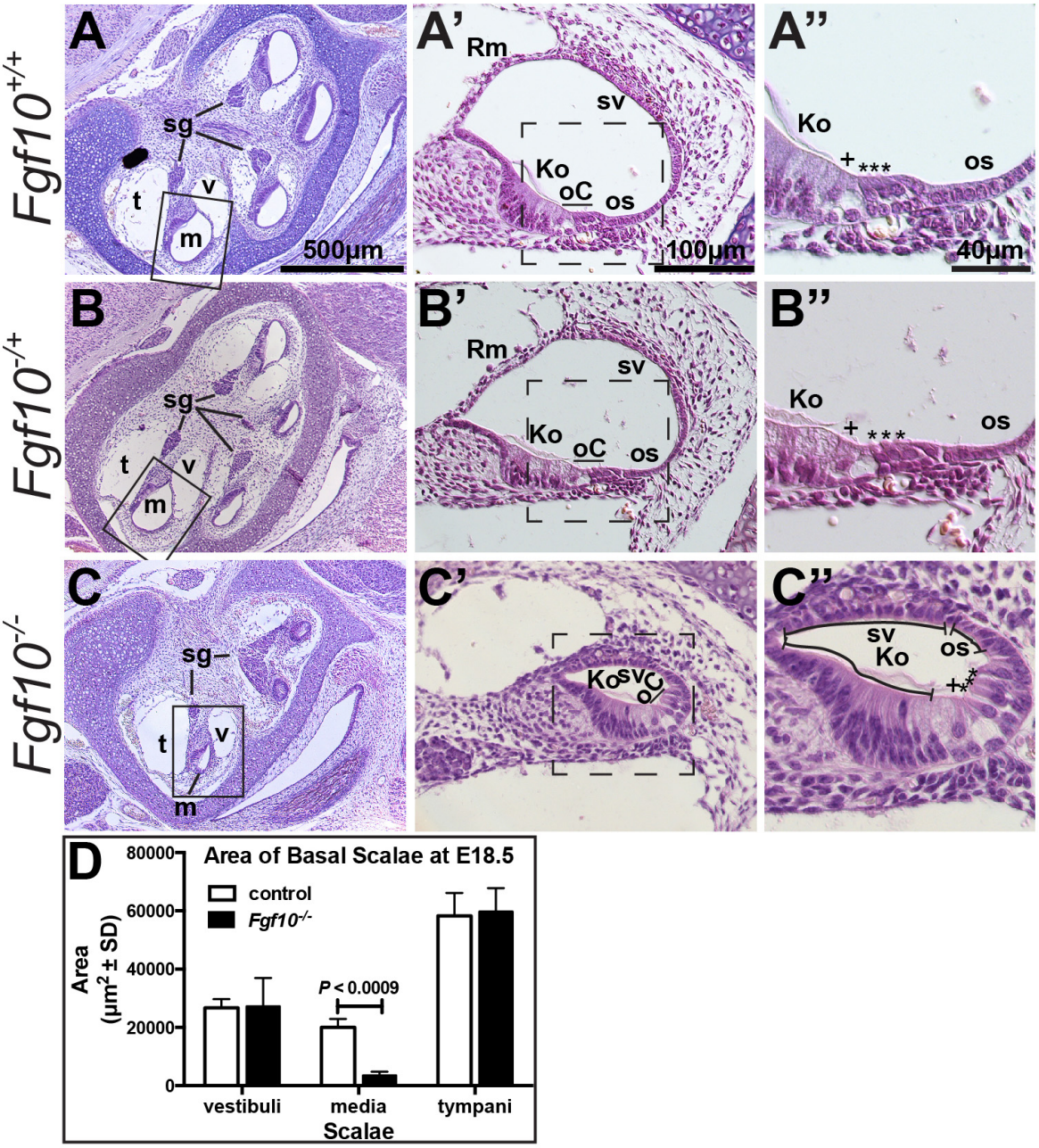

Figure 2. *Fgf10* null cochlear ducts lack non-sensory domains and have a reduced cross-sectional area. Hematoxylin and eosin-stained E18.5 cochlear duct cross sections at three magnifications. Boxes in A-C indicate the region magnified in A'-C'. Dashed boxes in A'-C'; indicate the region magnified in A"-C". C" Morphologic structures remaining in *Fgf10* mutants are indicated with lines. Genotypes are indicated to the left of each row. D. Graphical comparison of the cross sectional area of basal scalae (n = 3 controls and 3 mutants). Abbreviations: Ko, Kolliker's organ; m, scala media (cochlear duct), oC, organ of Corti; os, outer sulcus; Rm, Reissner's membrane; sg, spiral (cochlear) ganglion; sv, stria vascularis; t, scala tympani; v, scala vestibuli. Asterisks indicate outer hair cells, plus symbols indicate inner hair cells. Scale bars in A, A', A'' apply to all panels in the same column.

UU IR Author Manuscript

Figure 3

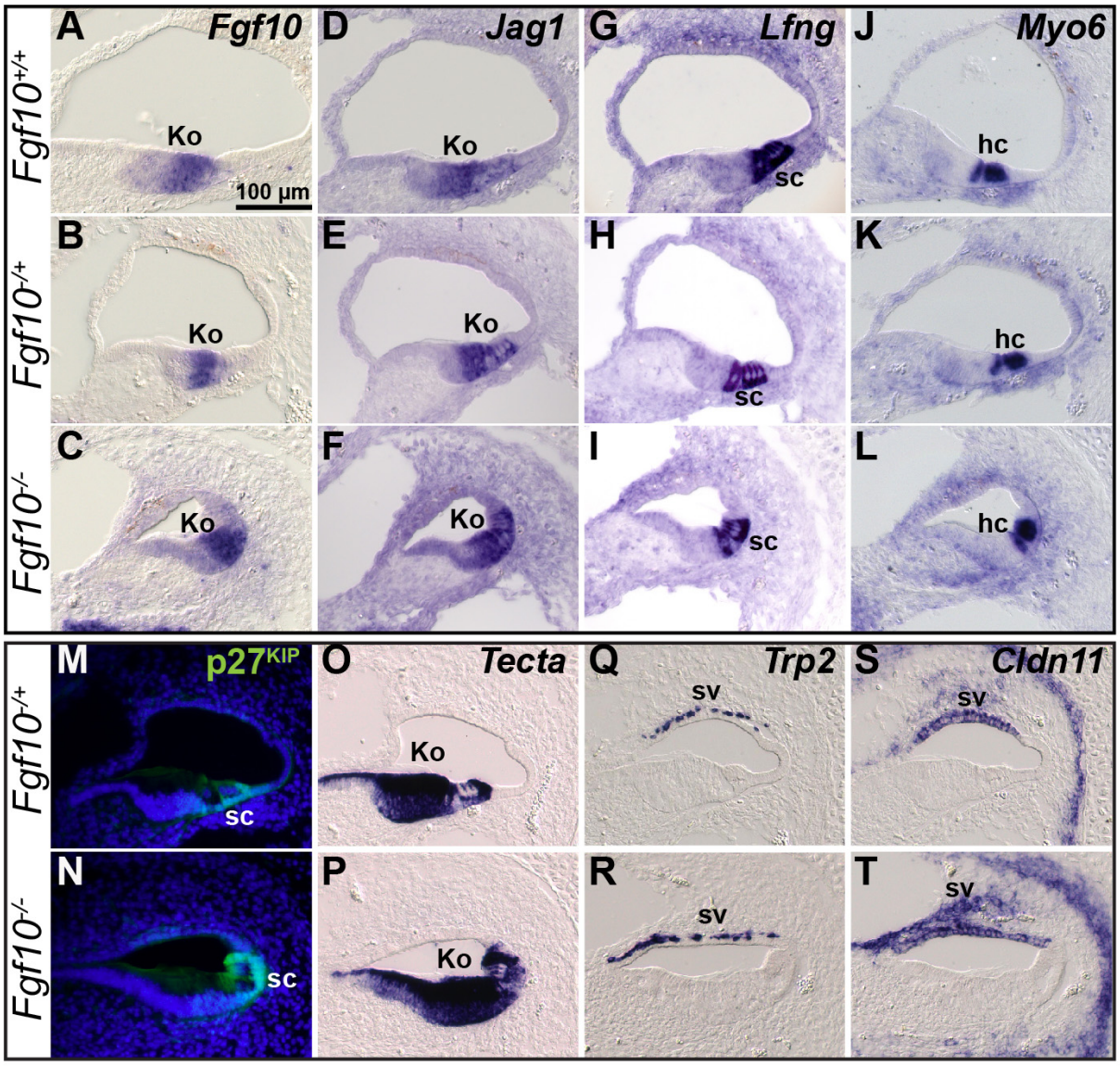

Figure 3. Markers of Kolliker's organ, supporting cells, hair cells and the stria vascularis are unchanged in E18.5 *Fgf10* null mutants. In situ hybridization (A-L, O-T) or immunostaining analysis (M, N) of cochlear cross sections. Genotypes are indicated to the left of each row and probes are indicated at the upper right of the top panel in each series. Abbreviations: hc, hair cells; Ko, Kolliker's organ; sc, supporting cells; sv, stria vascularis. Scale bar in A applies to all panels.

UU IR Author Manuscript

Figure 4

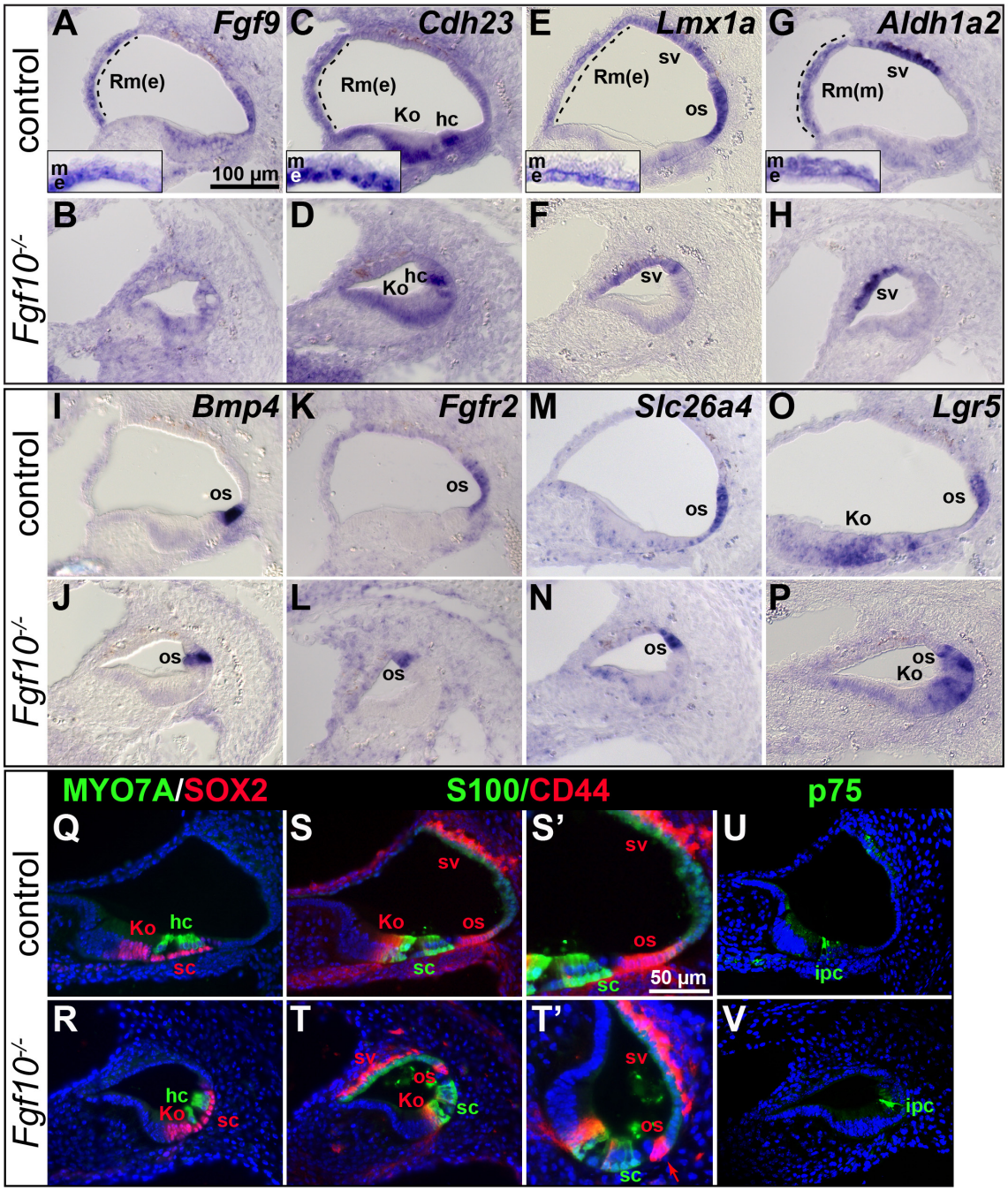

Figure 4. Markers of Reissner's membrane are absent and outer sulcus markers show a reduced domain in E18.5 *Fgf10* null mutant cochleae. In situ hybridization (A-P) and immunostaining (Q-V) analyses of basal cochlear duct cross sections. Genotypes are indicated to the left of each row and probes are indicated to the upper right of each pair of panels. Insets in A, C, E, G show magnifications of Reissner's membrane. S'-T' provide enlargements of S-T, with the arrow in T' indicating the remnant Claudius cells in the mutant os. Abbreviations: Rm(e), Reissner's membrane-epithelial layer; Rm(m), Reissner's membrane-mesenchymal/mesothelial domain; os, outer sulcus. See Figure 2 or 3 legend for others. Scale bar in A applies to all panels except S'-T'. Scale bar in S' applies to T'.

Figure 5

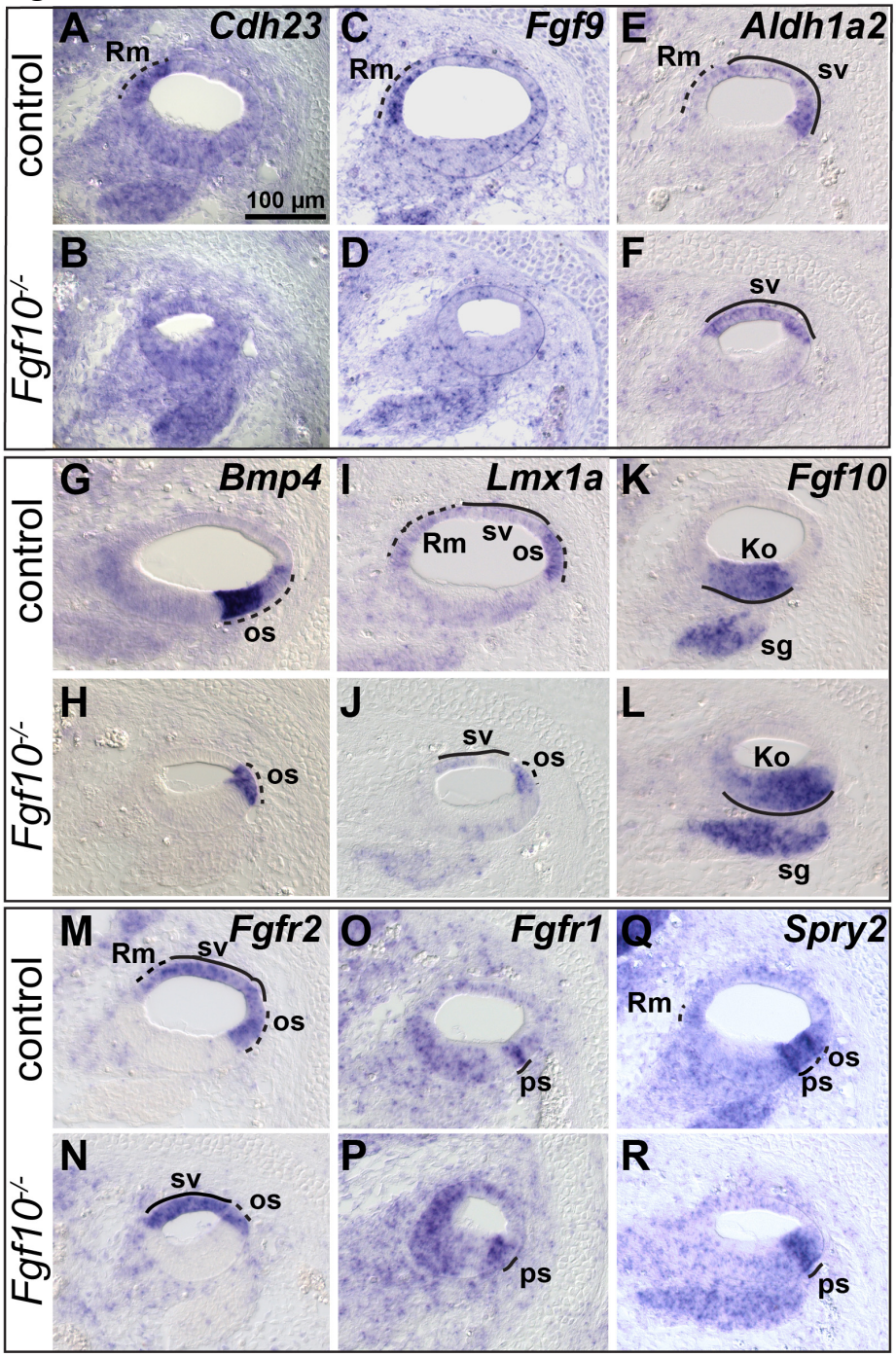

Figure 5. Presumptive Reissner's membrane markers are absent and presumptive outer sulcus markers show a reduced domain in E15.5 *Fgf10* null mutant cochleae. In situ hybridization analyses of basal cochlear duct cross sections are shown. Genotypes are indicated to the left of each row and probes are indicated to the upper right of each pair of panels. Dashed and solid lines indicate expression that is altered or unchanged, respectively, in mutants. Abbreviations: Ko, presumptive Kolliker's organ; os, presumptive outer sulcus; ps, presumptive prosensory domain; Rm, presumptive Reissner's membrane; sg, spiral ganglion; sv, stria vascularis. Scale bar in A applies to all panels.

Figure 6

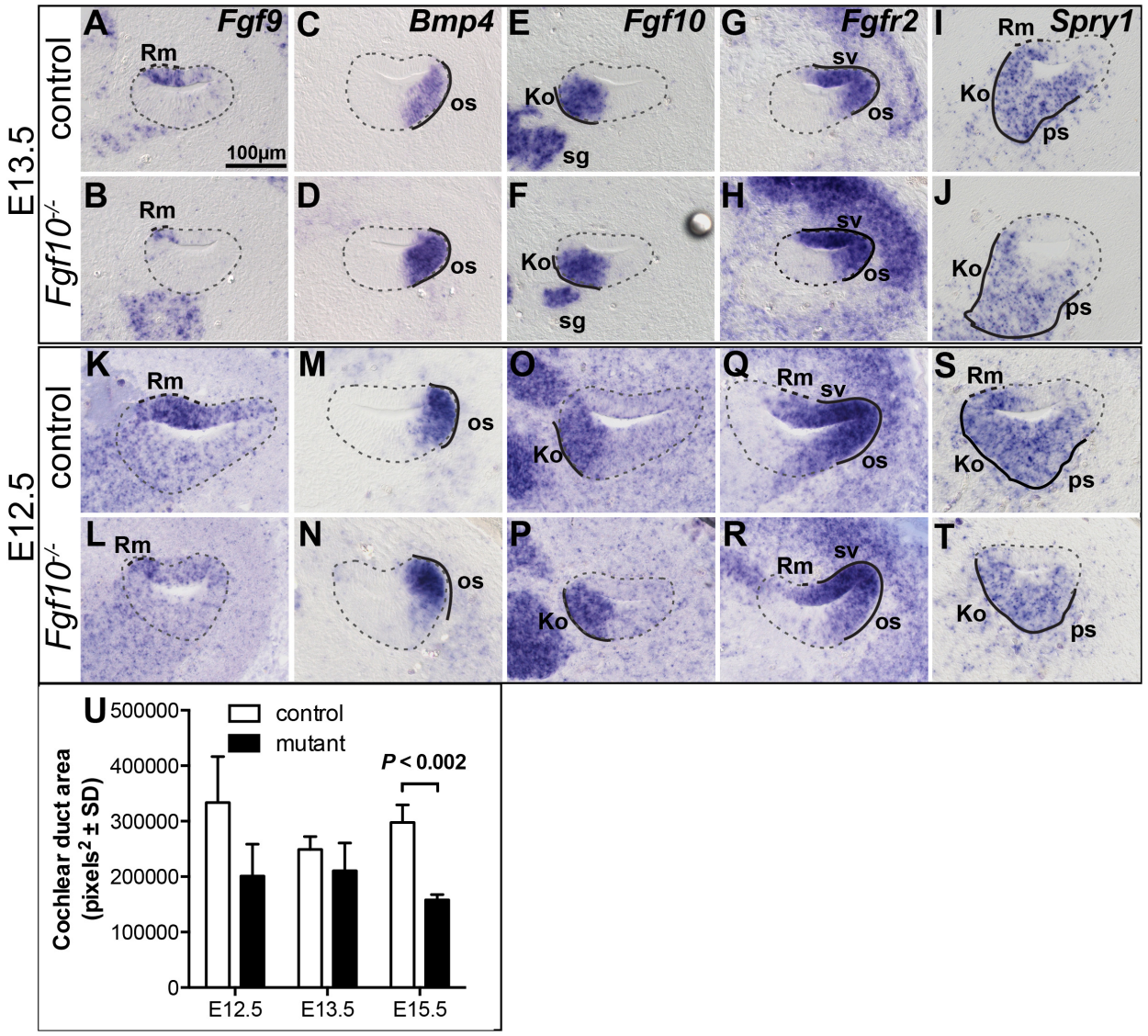

Figure 6. The effects of FGF10 absence on Reissner's membrane development precede those on outer sulcus development. In situ hybridization analyses of basal cochlear duct cross sections at E13.5 (A-J) and E12.5 (K-T). Genotypes are indicated to the left of each row and probes are indicated to the upper right of the top panels. Dashed and solid black lines indicate expression that is altered or unchanged, respectively, in mutants. The cochlear duct is outlined with a dashed grey line. U. Graphical comparison of the cochlear duct area of the basal scala media at the developmental ages shown (n = 3 controls and 3 mutants). Abbreviations: Ko, Kolliker's organ; Rm, presumptive Reissner's membrane; os, outer sulcus; ps, prosensory region; sg, spiral ganglion; sv, stria vascularis. Scale bar in A applies to all panels.

UU IR Author Manuscript

Figure 7

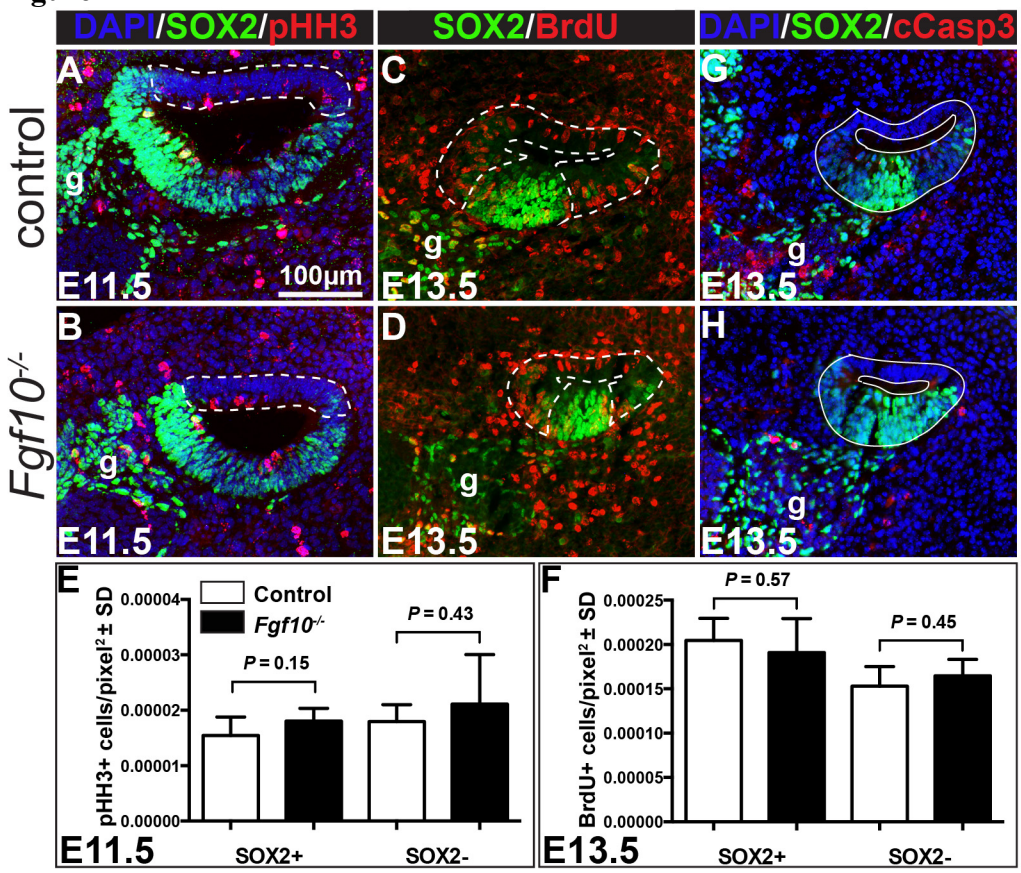

Figure 7. Neither cell proliferation nor cell survival is altered in *Fgf10* null cochlear ducts. Double labeling of control (A) and *Fgf10* null (B) E11.5 cochlear duct cross sections with antibodies directed against phospho-Histone H3 (red) and SOX2 (green). Nuclei are counterstained with DAPI (blue). Double labeling of control (C) and *Fgf10* null (D) E13.5 cochlear duct cross sections with antibodies directed against BrdU (red) and SOX2 (green). Dotted lines delineate the regions considered non-sensory (SOX2-). The remaining SOX2+ areas were considered prosensory. Graphical comparisons of the mean number of proliferating cells per pixel^2 in SOX2+ (E) and SOX2- (F) regions of control (white bars) and *Fgf10* null mutants (black bars). Error bars indicate standard deviation (SD). Double labeling of control (G) and *Fgf10* null (H) E13.5 cochlear duct cross sections with antibodies directed against cleaved Caspase 3 (cCasp3; red) and SOX2 (green). Nuclei are counterstained with DAPI (blue). Abbreviation: g, ganglion. Scale bar in panel A applies to all images.

Figure 8

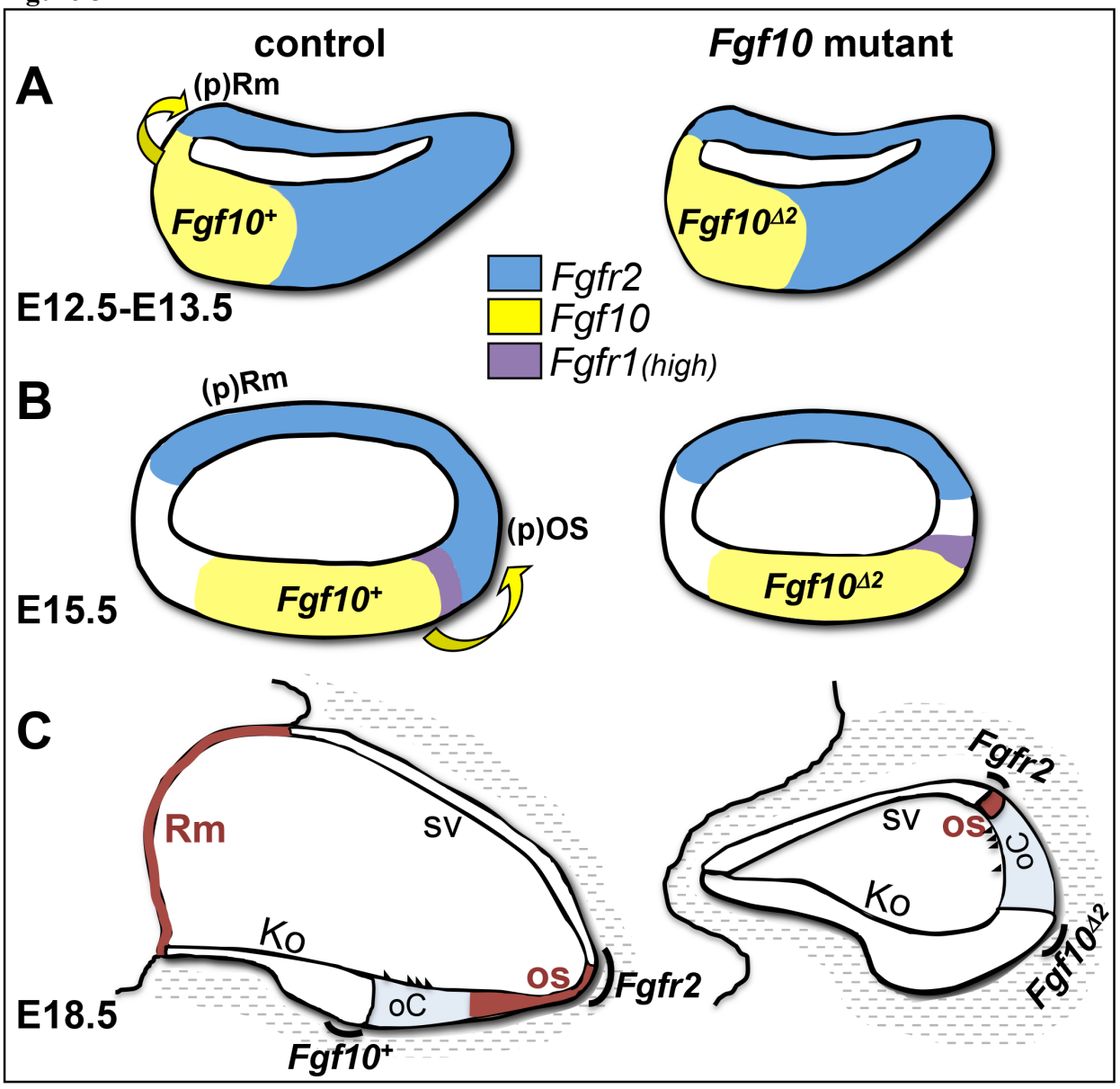

Figure 8. Model depicting the effects of FGF10 absence on development of non-sensory cochlear domains. (A) At E12.5-E13.5 FGF10 induces Reissner's membrane development at the medial boundary of *Fgf10/Fgfr2* expression. (B) By E15.5, FGF10 induces outer sulcus development at the lateral boundary of *Fgf10/Fgfr2* expression. Expression domains of *Fgf10* and receptor genes are color coded in A and B. (C) Failure of FGF10 signaling leads by E18.5 to a total loss of Reissner's membrane and a significant reduction in the outer sulcus. Both affected domains are colored brown. Other morphologic domains are delineated and the now quite separated expression domains for *Fgf10* and *Fgfr2* are indicated with black arcs. There is low-level diffuse expression of *Fgfr1* throughout much of the cochlear duct at all stages (not shown). *Fgf10*$^{\Delta 2}$ refers to the stable exon 2-deleted transcript that does not encode functional FGF10, but perdures in the mutant. All other abbreviations have been defined previously.

UU IR Author Manuscript

Supplementary Table 1

cDNA clones used to prepare digoxigenin-labeled cRNA antisense transcripts for in situ hybridization

Gene	Insert size	Enzyme	Polymerase	Source	Reference
Bmp4	~900 bp	Acc1	T7	Anne Boulet	Jones et al., 1991
Cldn11	~1.8 kb	NcoI	T3	Andreas Kispert	Trowe et al., 2011
Fgf9	~860 bp	HindIII	SP6	David Ornitz via Sabine Fuhrmann	Colvin et al., 1999
Fgf10	~550 bp	EcoR1	SP6	David Ornitz	Xu et al., 1998
Fgfr1	459 bp	EcoRI	T7	GenBank BC010200	Li et al., 2007
Fgfr2	~1.8 kb	EcoRI	SP6	Olivia Bermingham-McDonogh	Hayashi et al., 2010
Lfng	~1 kb	HindIII	T3	Doris Wu	Morsli et al., 1998
Myo6	834 bp	NotI	T7	Karen Avraham	Avraham et al., 1995
Spry1	~1.5 kb	EcoRI	T7	Kathy Shim	Minowada et al., 1999
Spry2	~1.5 kb	XbaI	T3	Kathy Shim	Minowada et al., 1999
Tecta	~4.5 kb	EcoRI	T7	Guy Richardson	Rau et al., 1999
Trp2	~1kb	HindIII	T7	Doris Wu	Morsli et al., 1999

Purified DNA was digested with the indicated restriction enzyme and then transcribed with the indicated RNA polymerase to produce antisense probes for in situ hybridization.

Reference List for Probes:

Avraham, K. B., Hasson, T., Steel, K. P., Kingsley, D. M., Russell, L. B., Mooseker, M. S., Copeland, N. G., Jenkins, N. A., 1995. The mouse Snell's waltzer deafness gene encodes an unconventional myosin required for structural integrity of inner ear hair cells. Nat Genet. 11**,** 369-375.

Colvin, J. S., Feldman, B., Nadeau, J. H., Goldfarb, M., Ornitz, D. M., 1999. Genomic organization and embryonic expression of the mouse fibroblast growth factor 9 gene. Dev Dyn. 216**,** 72-88.

Hayashi, T., Ray, C. A., Younkins, C., Bermingham-McDonogh, O., 2010. Expression patterns of FGF receptors in the developing mammalian cochlea. Dev Dyn. 239**,** 1019-1026.

Jones, C. M., Lyons, K. M., Hogan, B. L., 1991. Involvement of Bone Morphogenetic Protein-4 (BMP-4) and Vgr-1 in morphogenesis and neurogenesis in the mouse. Development. 111**,** 531-542.

Li, C., Scott, D. A., Hatch, E., Tian, X., Mansour, S. L., 2007. Dusp6 (Mkp3) is a negative feedback regulator of FGF-stimulated ERK signaling during mouse development. Development. 134**,** 167-176.

Minowada, G., Jarvis, L. A., Chi, C. L., Neubuser, A., Sun, X., Hacohen, N., Krasnow, M. A., Martin, G. R., 1999. Vertebrate Sprouty genes are induced by FGF signaling and can cause chondrodysplasia when overexpressed. Development. 126**,** 4465-4475.

Morsli, H., Choo, D., Ryan, A., Johnson, R., Wu, D. K., 1998. Development of the mouse inner ear and origin of its sensory organs. J Neurosci. 18**,** 3327-3335.

Morsli, H., Tuorto, F., Choo, D., Postiglione, M. P., Simeone, A., Wu, D. K., 1999. Otx1 and Otx2 activities are required for the normal development of the mouse inner ear. Development. 126**,** 2335-2343.

Rau, A., Legan, P. K., Richardson, G. P., 1999. Tectorin mRNA expression is spatially and temporally restricted during mouse inner ear development. J Comp Neurol. 405**,** 271-280.

Trowe, M. O., Maier, H., Petry, M., Schweizer, M., Schuster-Gossler, K., Kispert, A., 2011. Impaired stria vascularis integrity upon loss of E-cadherin in basal cells. Dev Biol. 359**,** 95-107.

Xu, X., Weinstein, M., Li, C., Naski, M., Cohen, R. I., Ornitz, D. M., Leder, P., Deng, C., 1998. Fibroblast growth factor receptor 2 (FGFR2)-mediated reciprocal regulation loop between FGF8 and FGF10 is essential for limb induction. Development. 125**,** 753-765.

Supplementary Table 2

Primers used to generate DNA fragments for cRNA probe production

Gene	Primers	Primer sequences (5'-3')	Product size (bp)
Cdh23	F-816	CAAGATGGAATCCACATGGTTCATGG	651
	R-817	ATGCTTTGTTCCCTCATCCACTGG	
Fgf16	F-832	TGTGACCCATGTACTCTGTGACC	457
	R-833	ACGAATGAGAGATCTGCAGAGCC	
Jag1	F-812	TGCTGAGCTCTGTCTTAACAGTGG	605
	R-813	ACAGAAACTACCAGTGCCAGTGG	
Lgr5	F-826	CCTATTTGGTAGCTGGCTGATCC	657
	R-827	AGCAACAGAGCAATGTGCTTCACC	
Lmx1a	F-828	TCAGTAACCTGGGAGACTGCTTCC	836
	R-829	GCCATCTGGAGTTGTATTCTAGACC	
Aldh1a2	F-810	CTCACAACAAGTGAGCTTCAGCC	407
	R-811	ACTGTAGGAGGAACAGAGAGCC	
Slc26a4	F-822	GTAGACTTGCTTCCTGAGAGAGG	448
	R-823	CACATGGATTTCAGAGTCAGTCAGG	

Forward (F) and reverse (R) primers used to PCR-amplify 3'UTR regions of each indicated gene from mouse genomic DNA. All reverse primers include the T7 promoter sequence (GGATCCTAATACGACTCACTATAGGGAG) at the 5' end. The antisense-RNA strand was produced by transcription of the PCR product using T7 RNA polymerase.

UU IR Author Manuscript

Supplementary Figure 1

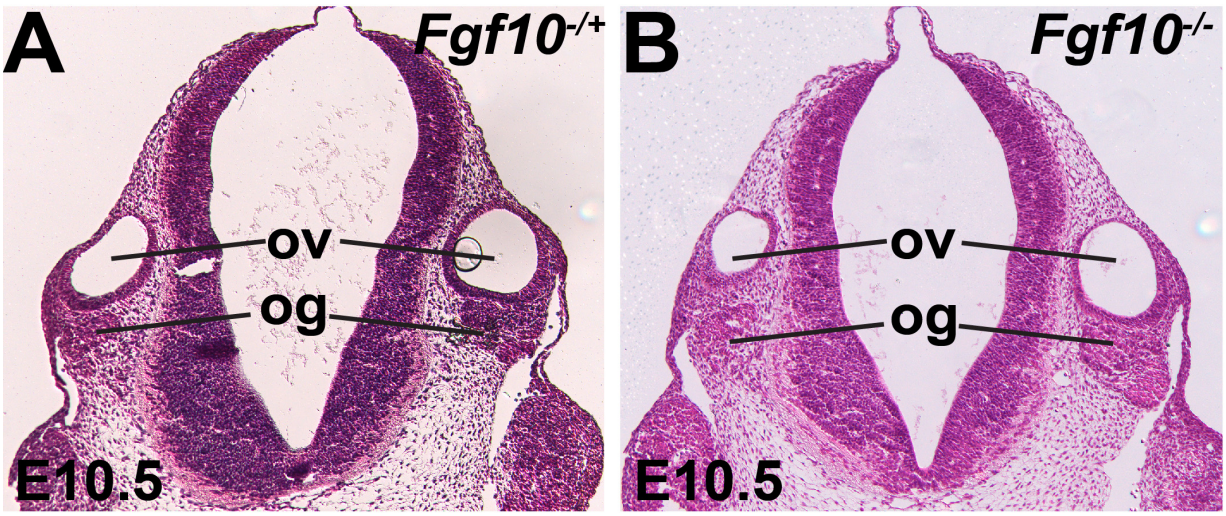

Figure S1. Otic development is normal in E10.5 *Fgf10* null mutants. Hematoxylin and eosin stained transverse sections of (A) heterozygous and (B) homozygous null *Fgf10* mutants show similar development of the otic vesicle (ov) and otic ganglion (og).

UU IR Author Manuscript

Supplementary Figure 2

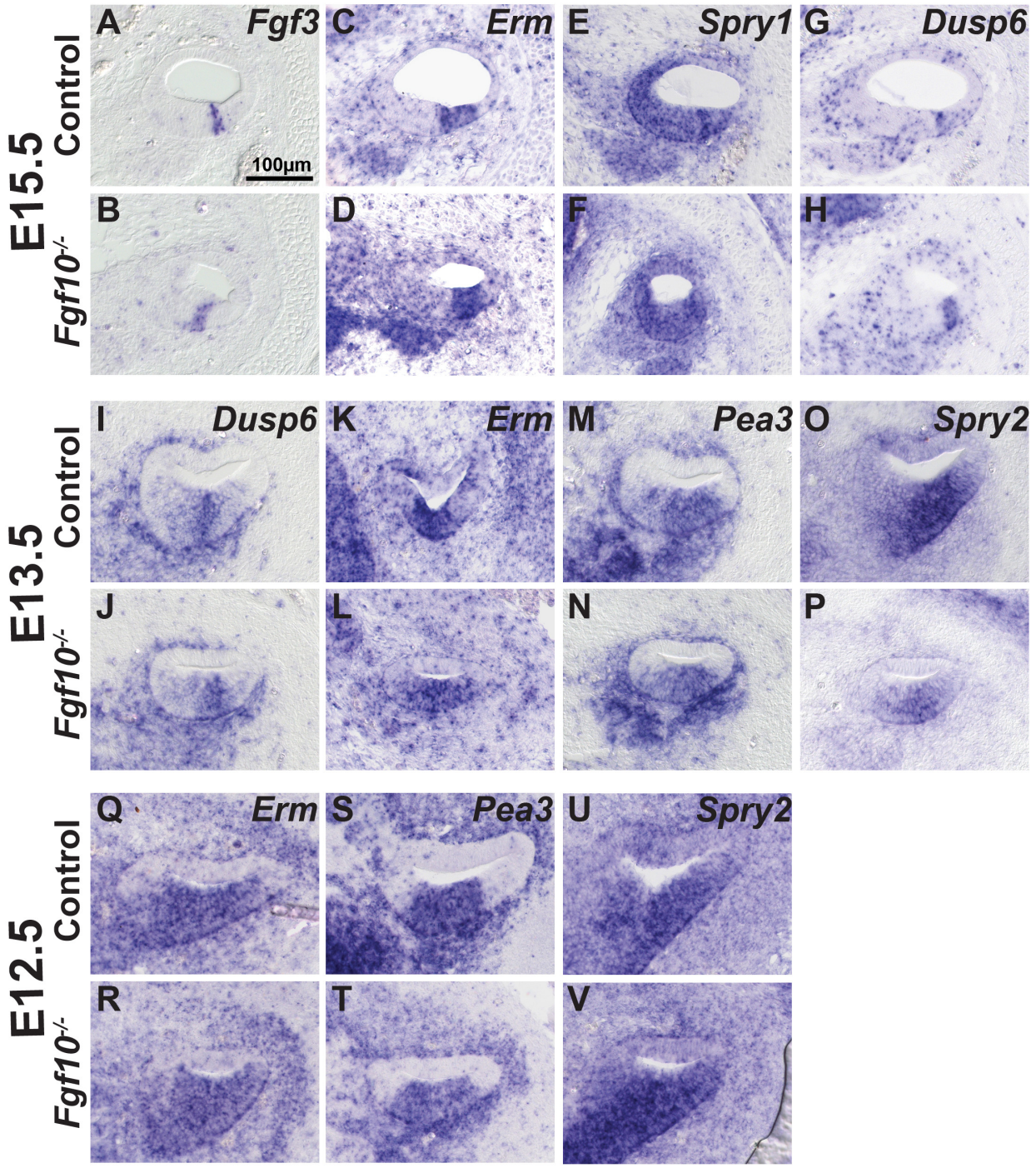

Figure S2. *Fgf3* and several FGF signaling indicators are expressed similarly in control and *Fgf10*$^{-/-}$ embryos. Cochlear duct cross sections at the stages indicated to the left were hybridized with the indicated probes. The scale bar in A applies to all panels.